ORGAN TOXICITY AND MECHANISMS

Comparative metabolism of aflatoxin B$_1$ in mouse, rat and human primary hepatocytes using HPLC–MS/MS

Andrea Gerdemann[1] · Benedikt Cramer[1] · Gisela H. Degen[2] · Jannik Veerkamp[1] · Georgia Günther[2] ·
Wiebke Albrecht[2] · Matthias Behrens[1] · Melanie Esselen[1] · Ahmed Ghallab[2,3] · Jan G. Hengstler[2] ·
Hans-Ulrich Humpf[1]

Abstract

Aflatoxin B$_1$ (AFB$_1$) is a highly hepatotoxic and carcinogenic mycotoxin produced by *Aspergillus* species. The compound is mainly metabolized in the liver and its metabolism varies between species. The present study quantified relevant AFB$_1$-metabolites formed by mouse, rat, and human primary hepatocytes after treatment with 1 μM and 10 μM AFB$_1$. The use of liquid chromatographic separation coupled with tandem mass spectrometric detection enabled the selective and sensitive determination of phase I and phase II metabolites of AFB$_1$ over incubation times of up to 24 h. The binding of AFB$_1$ to macromolecules was also considered. The fastest metabolism of AFB$_1$ was observed in mouse hepatocytes which formed aflatoxin P$_1$ as a major metabolite and also its glucuronidated form, while AFP$_1$ occurred only in traces in the other species. Aflatoxin M$_1$ was formed in all species and was, together with aflatoxin Q$_1$ and aflatoxicol, the main metabolite in human cells. Effective epoxidation led to high amounts of DNA adducts already 30 min post-treatment, especially in rat hepatocytes. Lower levels of DNA adducts and fast DNA repair were found in mouse hepatocytes. Also, protein adducts arising from reactive intermediates were formed rapidly in all three species. Detoxification via glutathione conjugation and subsequent formation of the *N*-acetylcysteine derivative appeared to be similar in mice and in rats and strongly differed from human hepatocytes which did not form these metabolites at all. The use of qualitative reference material of a multitude of metabolites and the comparison of hepatocyte metabolism in three species using advanced methods enabled considerations on toxification and detoxification mechanisms of AFB$_1$. In addition to glutathione conjugation, phase I metabolism is strongly involved in the detoxification of AFB$_1$.

Keywords Mycotoxins · DNA adducts · Protein adducts · Species differences · HPLC–MS/MS · Biotransformation

✉ Hans-Ulrich Humpf
humpf@uni-muenster.de

Andrea Gerdemann
andrea.gerdemann@uni-muenster.de

[1] Institute of Food Chemistry, University of Münster, Corrensstraße 45, 48149 Münster, Germany

[2] Leibniz Research Centre for Working Environment and Human Factors (IfADo), Ardeystraße 67, 44139 Dortmund, Germany

[3] Department of Forensic Medicine and Toxicology, Faculty of Veterinary Medicine, South Valley University, Qena 83523, Egypt

Introduction

Aflatoxin B$_1$ (AFB$_1$) is a well-known secondary metabolite mainly produced by *Aspergillus flavus* and *Aspergillus parasiticus* (Dohnal et al. 2014). These fungal species grow on various crops, especially in warm regions with high humidity, which are therefore highly endangered for aflatoxin contamination in food and feed (Rushing and Selim 2019). The compound is highly toxic and carcinogenic related to a mutagenic mode of action (Kensler et al. 2011) and toxicological properties, summarized in a recent opinion from the European Food Safety Authority (EFSA CONTAM PANEL 2020). The metabolism of AFB$_1$ varies among species, which is known from early in vitro experiments using microsomes (Moss et al. 1985; Ramsdell and Eaton 1990; Yourtee et al. 1987; Roebuck and Wogan 1977) and studies

reviewed elsewhere (Dohnal et al. 2014; Rushing and Selim 2019). As depicted in Fig. 1, AFB$_1$ is metabolized by cytochrome P450 enzymes (CYP), which catalyze demethylation to aflatoxin P$_1$ (AFP$_1$), hydroxylation to aflatoxin M$_1$ (AFM$_1$) and aflatoxin Q$_1$ (AFQ$_1$) or epoxidation of the compound (Deng et al. 2018; Ramsdell and Eaton 1990). Also, the formation of aflatoxicol (AFL) upon reduction of AFB$_1$ is a well-known metabolic step (Wong et al. 1979). Most phase I metabolites such as AFP$_1$, AFM$_1$, AFQ$_1$, and AFL exert lower cytotoxicity than AFB$_1$ (Buchi et al. 1973; Green et al. 1982; Neal et al. 1998; Wu et al. 2021; Yourtee et al. 1987). In contrast, the *exo*-epoxide is a highly reactive intermediate which binds covalently to the guanine residue of DNA (van Vleet et al. 2002; Hanigan and Laishes 1984). This bioactivation reaction is considered critical for the mutagenicity and carcinogenicity of AFB$_1$ (Eaton and Gallagher 1994; Essigmann et al. 1977). The AFB$_1$-guanine adduct can be converted to a rather persistent formamidopyrimidine (FAPY) adduct which is mainly responsible for the mutagenicity of AFB$_1$ since the guanine adduct is repaired more efficiently (Smela et al. 2002).

The main mechanism for detoxification of the epoxide is the conjugation with glutathione (GSH) to an AFB$_1$-GSH adduct which is further metabolized to the *N*-acetylcysteine (NAC) derivative (Moss et al. 1985; Degen and Neumann 1978; Raj and Lotlikar 1984). The toxicity of AFB$_1$ in various species is therefore related to the efficiency of this detoxifying conjugation reaction (Murcia and Diaz 2021; Degen and Neumann 1981; Ilic et al. 2010). Furthermore, the epoxide is rapidly hydrolyzed to AFB$_1$-dihydrodiol which is in equilibrium with the reactive AFB$_1$-dialdehyde (Neal and Colley 1979). To what extent this hydrolysis is catalyzed by epoxide hydrolases or if it is spontaneously generated due to the instability of the compound is under discussion (Guengerich et al. 1998; Johnson et al. 1997). Nevertheless, the formed dialdehyde can further react with primary amines such as the ε-amino group of lysine present in serum albumin, which makes the determination of AFB$_1$-lysine (AFB$_1$-Lys) adducts in blood samples a reliable long-term biomarker for AFB$_1$ exposure (Sabbioni et al. 1987; Wild et al. 1990).

So far, the metabolism of AFB$_1$ is already relatively well described, but comprehensive quantitative data covering a broad spectrum of metabolites are still lacking. Therefore, the present investigation focused on species differences in AFB$_1$ metabolism between rats, mice, and humans using primary hepatocytes. The absolute quantification of main metabolites, in addition to the analysis of DNA and protein
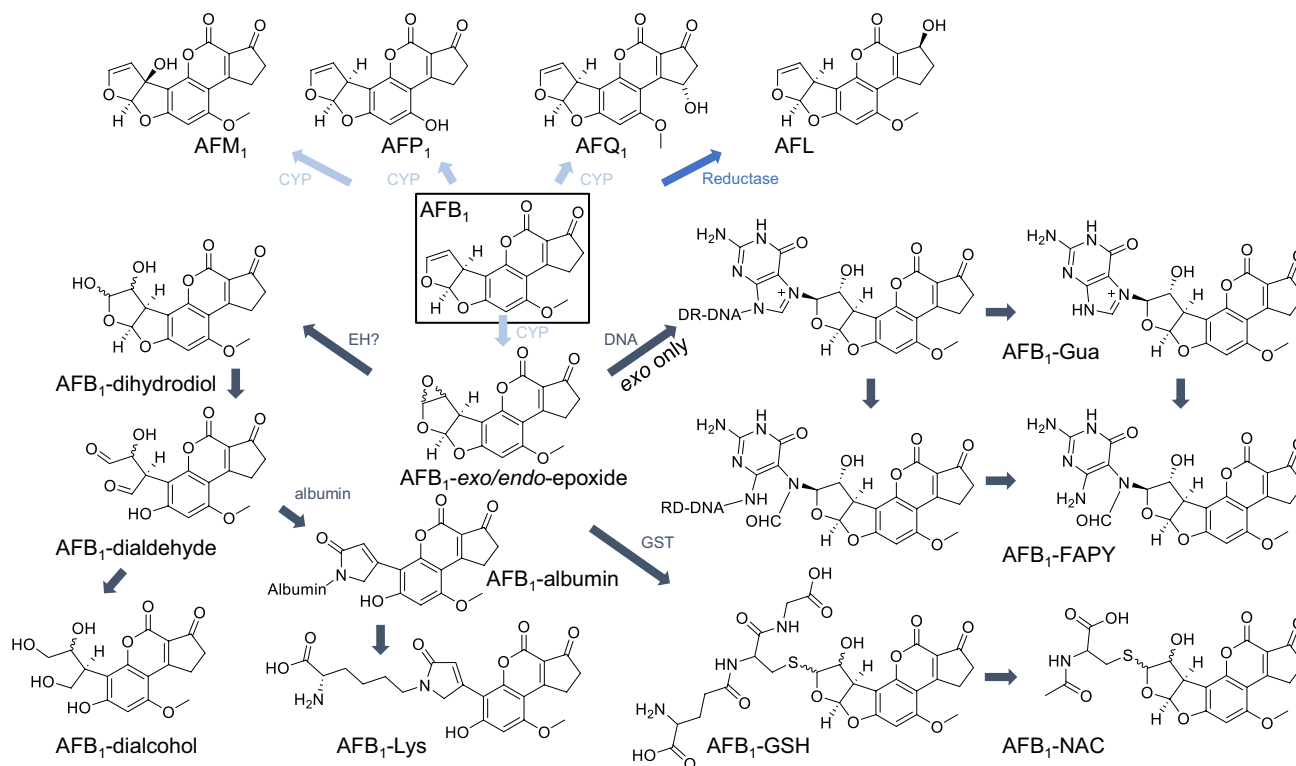

Fig. 1 Phase I metabolism of AFB$_1$ to AFM$_1$, AFP$_1$, AFQ$_1$, and AFL. AFB$_1$-epoxide binds to macromolecules such as proteins and DNA. Their downstream products AFB$_1$-Lys and AFB$_1$-Gua are used as long- and short-term biomarkers for AFB$_1$ exposure. Efficient detoxi-fication via glutathione conjugation reduces adduct formation (*EH* epoxide hydrolase, *GST* glutathione-*S*-transferase, *CYP* cytochrome P450)

adducts at specific time points, gives a comprehensive metabolism kinetics of AFB_1 in these species. The synthesis of reference compounds enabled the quantification of AFB_1 adducts, which are not commercially available.

Materials and methods

Chemicals and reagents

Solvents and chemicals were purchased from Fisher Scientific (Schwerte, Germany), Carl Roth (Karlsruhe, Germany), Sigma-Aldrich (Steinheim, Germany), or VWR (Darmstadt, Germany) if not further specified. Water was purified via the PureLab Flex2 system (Veolia Water Technologies, Celle, Germany). AFB_1 (purity ≥ 98%, Sigma-Aldrich), AFM_1 (purity ≥ 95%, Enzo Life Sciences, Lörrach, Germany), AFP_1 (TRC, Toronto, Canada), AFQ_1 and AFL (purity > 98%, Biomol, Hamburg, Germany) were commercially available as reference compounds and their concentration was adjusted gravimetrically. Solvents were used in LC–MS grade.

Synthesis and purification of reference compounds

AFB₁-epoxide

The epoxidation of AFB_1 was induced by a reaction with dimethyldioxirane (DMDO), which was synthesized according to a previously reported method based on the reaction of acetone with potassium peroxymonosulfate (Taber et al. 2013; Sass et al. 2013). The concentration of DMDO was determined via iodometric titration just before use. 0.06 mmol of AFB_1 was dissolved in 3 mL of dichlormethane and 0.09 mmol of DMDO was added. The solution was stirred for 15 min at room temperature and the solvent as well as the remaining DMDO were evaporated afterwards. The residue, containing the AFB_1-epoxide, was reconstituted in 1.1 mL dimethylsulfoxide (DMSO).

AFB₁-N^7-guanine

For the synthesis of AFB_1-N^7-guanine (AFB_1-Gua), based on previous reports (Vidyasagar et al. 1997), 0.12 mmol guanine was added to the solution containing 0.06 mmol of AFB_1-epoxide in 1.1 mL DMSO and stirred for 15 min at room temperature. The product was purified using a Bond Elute PRS solid phase extraction (SPE) cartridge (1 mg, 6 mL, Agilent, Waldbronn, Germany). After washing with 2% formic acid (FA) and pure methanol (MeOH), the compound was eluted with 5% ammonium hydroxide in MeOH. The adduct was purified using preparative high-performance liquid chromatography coupled to an ultraviolet detector

(HPLC–UV) (365 nm) on a Nucleodur Phenyl-Hexyl column (250 × 4 mm, 5 µm, Macherey–Nagel, Düren, Germany) and an acetonitrile (ACN)/water gradient supplemented with 0.1% FA. Because of the low yield of the synthesis the concentration of the final solution was determined photometrically based on a molar extinction coefficient of 18.000 L/mol/cm (362 nm) in 0.05 M phosphate buffer (pH 7.0) (Coskun et al. 2019). Further details on the purification steps are shown in Online Resource 1 (Tables S1 and S2).

AFB₁-formamidopyrimidine

Parts of the purified AFB_1-Gua were used to synthesize the AFB_1-FAPY guanine (Alekseyev et al. 2004). Therefore, an aliquot of the AFB_1-Gua solution was alkalized to pH 10–11 with 0.1 M sodium hydroxide (NaOH) and shaken for 4 h at 37 °C. Because of the low amounts of starting material, just a qualitative standard was synthesized without further purification.

AFB₁-lysine

The synthesis of AFB_1-Lys was carried out in parallel to the AFB_1-Gua synthesis. The two washing phases from the SPE clean-up of AFB_1-Gua were used separately as starting material as the lysine adduct is formed from AFB_1-dialdehyde and AFB_1-dihydrodiol which eluted in these steps. The first washing phase was diluted with phosphate buffer and the second washing phase was evaporated to dryness and the residue was also reconstituted in phosphate buffer (0.1 M, pH 7.4). Two equivalents of N_α-Boc-L-lysine (0.12 mmol, Alfa Aesar, Kandel, Germany), protected at the α-amino group, were added to both solutions and stirred at room temperature in the dark for about 22 h.

The samples were purified on a Strata-X (1 g, 12 mL, Phenomenex, Aschaffenburg, Germany) SPE cartridge and AFB_1-Boc-lysine was eluted with water and 50% MeOH during the washing steps. For further preparative purification using HPLC–UV (399 nm), a Nucleodur Phenyl-Hexyl column (250 mm × 4 mm, 5 µm) and a gradient of ACN and water with 0.1% FA were used. The Boc-protection group was removed by the addition of trifluoracetic acid followed by 18 h of stirring at room temperature in the dark. For the neutralization of the solution phosphate buffer (0.1 M, pH 7.4) and 10 M NaOH were added. For further purification, the same preparative HPLC method as applied for the purification of the Boc-lysine adduct was used. The concentration of the purified solution in 0.1 M phosphate buffer (pH 7.4) was determined photometrically with a molar extinction coefficient of 30 866 L/mol/cm (400 nm) (Renaud et al. 2022). A purity of 59.5% was determined using HPLC–DAD (diode-array detector). More details on the purification can be found in Online Resource 1 (Tables S3 and S4).

AFB$_1$-*N*-acetylcysteine

The *N*-acetylcysteine derivative was formed by a reaction of AFB$_1$-epoxide with *N*-acetylcysteine. Therefore, 20 equivalents of *N*-acetylcysteine (0.64 mmol, Alfa Aesar) were dissolved in phosphate buffer (0.1 M, pH 7.4), cooled to 5 °C and added to 0.032 mmol of AFB$_1$-epoxide within 10 min. The solution was stirred for 60 min at 5 °C. The included acetone was evaporated and the residue was purified with an SPE clean-up on a C18-E cartridge (2 g, 12 mL, Phenomenex). AFB$_1$-*N*-acetylcysteine (AFB$_1$-NAC) eluted with 10–20% of MeOH and the organic solvent of the combined phases was removed within 30 min at 30 °C *in vacuo* as the compound degrades easily. The remaining solution was lyophilized and further purified via preparative HPLC–UV (350 nm) on a Nucleodur Phenyl-Hexyl column (250 mm × 10 mm, 5 μm). A second purification step with a similar column but with a lower diameter (250 × 4 mm, 5 μm) was carried out afterward. In the following SPE purification with a Strata -X-33 μm (100 mg, 3 mL, Phenomenex), the compound was eluted with 100% of MeOH, and the solution was directly used for the photometric quantification on the base of a molar extinction coefficient of 20 000 L/mol/cm (Moss et al. 1985). A purity of 100% was determined using HPLC–DAD (365 nm). Further details are shown in Online Resource 1 (Tables S5 and S6).

AFB$_1$-glutathione

The glutathione derivative was synthesized enzymatically using rat liver microsomes, and cytosol as initial experiments indicated higher yields of AFB$_1$-glutathione compared to the non-enzymatic reaction of glutathione (GSH) with AFB$_1$-epoxide. A solution containing 5 mM GSH, 0.5 mM AFB$_1$, and 0.1 M phosphate buffer (pH 7.4) (similar to Moss et al. 1983) was supplemented with rat liver microsomes and rat liver cytosol to protein contents of 5.25 mg/mL and 7.9 mg/mL, respectively. Furthermore, 10 mM glucose 6-phosphate, 664 μM nicotinamide adenine dinucleotide phosphate (NADP$^+$), and 2 U/mL glucose 6-phosphate dehydrogenase were used. The reaction was carried out in 62 preparations of 1 mL each, as an upscaling reduced reaction yield. The suspension was shaken for 4 h at 37 °C followed by the addition of two equivalents of ice-cold ACN to stop the reaction. The proteins precipitated and the samples were centrifuged at 3000 × g at 20 °C. An SPE clean-up of the upper phase on a Strata C18-E SPE cartridge (2 g, 12 mL, Phenomenex) followed and the adduct was eluted with 20–30% of MeOH. The compound was further purified using preparative HPLC–UV (360 nm) on a Nucleodur Phenyl-Hexyl column (250 mm × 4 mm, 5 μm). The purified product was quantified photometrically in 0.1 M phosphate buffer (pH 7.4) based on an extinction coefficient of 21 800 L/mol/cm (Degen and Neumann 1978; McHugh et al. 1996). A purity of 100% was determined using HPLC–DAD (360 nm). Further details are presented in Online Resource 1 (Tables S7 and S8).

Characterization of reference compounds

All synthesized and purified reference compounds were characterized based on exact mass and fragmentation spectra, which are shown in Online Resource 1. An HPLC-qToF-MS coupling was used including an Elute pump (Bruker Daltonics, Bremen, Germany), a column oven (Bruker Daltonics) set to 40 °C, and a PAL HTC-xt autosampler (CTC Analytics, Zwingen, Switzerland) cooled to 8 °C. Furthermore, an Impact II with an Apollo II ESI source (Bruker Daltonics) was selected for mass spectrometric detection. The chromatographic separation was carried out on a Nucleodur C18 Pyramid column (100 × 2 mm, 3 μm, Macherey–Nagel) with an ACN/water gradient supplemented with 0.1% FA. The detailed gradient, further mass spectrometric parameters, and fragmentation data are shown in Online Resource 1 (Tables S9 and S10, Figures S1-S5). The same instrument setup and separation method coupled to a DAD (Bruker Daltonics) were used for the purity check.

Primary hepatocyte culture

Hepatocytes were isolated from male Wistar rats (180–200 g, Charles River, Sulzfeld, Germany) and from 8- to 12-week-old male C57BL/6N mice by using a previously described two-step perfusion procedure (Godoy et al. 2013, Appendix 1). The liver perfusions of rats and mice to isolate hepatocytes were approved by the local authorities. The freshly isolated primary rodent hepatocytes were used for plating on cell culture dishes, precoated with collagen from rat tail tendon, and then kept in sandwich culture as described before in detail (Godoy et al. 2013; Appendix 2). In brief, rat hepatocytes were seeded at a density of 1×10^6 cells/well, and mouse hepatocytes were seeded at 0.85×10^6 cells/well in 6-well plates on collagen from rat tail tendon (Roche, Basel, Switzerland) in 2 mL Williams E medium (Pan-biotech, Aidenbach, Germany), which was supplemented with L-glutamine (PAN-biotech) as well as penicillin, streptomycin, and gentamycin as antibiotics (PAN-biotech). A mixture of insulin, transferrin, and selenium (Sigma-Aldrich) as well as dexamethasone (Sigma-Aldrich) was also added. After 3 h of plating, the second collagen layer was added and incubated for 30 min. After complete gelation of collagen, cell cultures were treated with 1 μM and 10 μM AFB$_1$, respectively. The two concentrations were chosen to avoid cytotoxic effects but enable also the detection of metabolites formed in low yields.

Cryopreserved human hepatocytes from three donors purchased from Lonza (Basel, Switzerland) and Biovit (Brussels, Belgium) were also seeded on collagen-coated dishes at a density of 1×10^6 cells/well. 24 h after initial seeding, the human hepatocytes in sandwich culture were incubated with AFB_1 at 1 μM in triplicate, while two biological replicates were treated with 10 μM AFB_1.

Culture medium samples of rat, mouse, and human hepatocytes were withdrawn in duplicate at 10 min, 30 min, 60 min, 2 h, 4 h, 6 h, and 24 h after incubation with AFB_1 and were stored at -20 °C until HPLC–MS/MS analysis.

Determination of macromolecular adducts and intracellular metabolites

Additional wells were prepared for the determination of AFB_1 bound to macromolecules such as the DNA and proteins after 30 min, 2 h, and 24 h. Furthermore, the intracellular content of the analytes was determined in these samples. The isolation of the DNA was performed according to a modified protocol previously reported for the isolation of fungal DNA (Cenis 1992). The cells were washed twice with 2 mL of phosphate-buffered saline prior to adding 200 μL of lysis buffer (200 mM Tris(hydroxymethyl)aminomethane HCl (pH 8.5, Carl Roth), 0.25 M NaCl (Merck, Darmstadt, Germany), 0.025 M EDTA disodium salt (Carl Roth), and 0.5% sodium dodecyl sulfate (Carl Roth). A cell scraper was used for cell harvest and the lysate was transferred into a DNase-free reaction tube. The cells were resuspended and stored at -20 °C until further sample preparation. After thawing, 20 μL of proteinase K (2 mg/mL, Carl Roth) was added for protein digestion. The first replicate was digested at 58 °C for 90 min. As the high temperature turned out to cause adduct degradation, the digestions of the second and the third replicates were performed at room temperature. After protein digestion, 200 μL of potassium acetate (5 M, pH 7, Carl Roth) was added and the samples were centrifuged for 30 min ($14,840 \times g$, 4 °C). 1 mL isopropanol (-20 °C) was added to the supernatant and the samples were inverted until the DNA precipitated and the samples were centrifuged again (30 min, $14,840 \times g$, 4 °C).

The supernatant was diluted by a factor of 5 for the determination of intracellular AFB_1 and metabolite concentrations. 1 mL of the remaining supernatant was used to determine the formation of protein adducts by release and purification of AFB_1-lysine following a slight modification of the protocol published by McCoy et al. (2005). Therefore, isopropanol was evaporated and 500 μL of pronase (6.5 mg/mL in phosphate-buffered saline, Merck) supplemented with 10 μL of $^{13}C_6^{15}N_2$-AFB_1-Lys as stable isotope-labeled internal standard (10 ng/mL) was added. The samples were incubated at 37 °C overnight to ensure complete protein digestion. After centrifugation, the supernatant was purified and concentrated via SPE using a 1 cc Oasis MAX cartridge (Waters, Eschborn, Germany). AFB_1-Lys was eluted with 2% FA in MeOH, evaporated completely, and reconstituted in ACN/water (1 + 19, v/v) for the analysis. The detailed SPE cleanup method is provided in Online Resource 1 (Table S11).

The DNA pellet was washed with 500 μL of 70% ethanol and centrifuged (30 min, $14,840 \times g$, 4 °C). The supernatant was discarded and the DNA pellet was dried using a vacuum concentrator (10 mbar, 10 min, 1750 rpm, 40 °C). 100 μL of digestion buffer (10 mM Tris(hydroxymethyl) aminomethane, 5 mM $MgCl_2$, pH 7), which included 5 μL RNase (10 mg/mL, Sigma-Aldrich), was added to each sample and the RNA was digested overnight at 37 °C and gentle shaking. Afterward, 50 μL of potassium acetate was added and the DNA was precipitated with 500 μL isopropanol. Similar to the first precipitation the DNA was washed with 500 μL of 70% EtOH and dried under vacuum. After adding 100 μL of digestion buffer, the DNA was digested by 10 U DNase, 500 mU phosphodiesterase from *Crotalus adamanteus* venom, and 500 mU alkaline phosphatase from bovine intestinal mucosa (all from Sigma-Aldrich) at 37 °C and gentle shaking overnight. Subsequently, 200 μL of ACN was added (-20 °C) to precipitate the proteins and the samples were centrifuged (15 min, $14,840 \times g$, 4 °C). The supernatant was evaporated to dryness using a vacuum concentrator (10 mbar, 1750 rpm, 40 °C) and reconstituted in 50 μL water. An aliquot of the samples was diluted by a factor of 100 with water for the determination of 2´-deoxyguanosine.

Analysis of AFB_1 metabolites

All analytes, except intracellular AFB_1-Lys, were analyzed using HPLC–MS/MS on an Agilent Infinity 1260 HPLC system in combination with a QTRAP 6500 triple quadrupole mass spectrometer (SCIEX, Darmstadt, Germany). The analytes were separated using a Nucleodur C18 Pyramid column (150 mm × 2 mm, 3 μm, Macherey–Nagel). ACN (solvent A) and water (solvent B) both supplemented with 0.1% FA were used for gradient elution. In addition to the metabolites of AFB_1, 2´-deoxyguanosine (dG) was quantified in the DNA lysates to normalize AFB_1-Gua formation on DNA yield. AFB_1-Lys was analyzed using a QTRAP 7500 mass spectrometer (Sciex) in combination with an Agilent Infinity II Bio HPLC system. AFB_1-Lys was separated on a Reprosil-Pur C18 AQ HPLC column (150 × 2 mm, 3 μm, Dr. Maisch, Ammerbuch, Germany), also using an ACN/water gradient supplemented with 0.01% acetic acid. The injection volume and the dilution of the samples were selected according to the expected concentrations of the analytes. The samples were diluted with ACN/water (1 + 19, v/v). Detailed quantification data as well as further information

on HPLC and MS methods are summarized in the Online Resource 1 (Table S12-S20). Not detectable signals were set to zero for quantification. An overview of sample preparation procedures and the determination of metabolites in the different matrices is shown in Fig. 2.

Formation rates shown in Table S21 were calculated as a mean of the quotients of molar quantity and time. Only the time points representing a linear formation were included.

Results

The metabolism of AFB_1 was compared in three different mammalian systems: human, mouse, and rat. First, this study focused on the comparative analysis of the metabolism of AFB_1 in hepatocytes from two different rodent species. Primary hepatocytes from rats and mice were freshly isolated and treated with 1 μM and 10 μM of AFB_1 for up to 24 h. Additionally, cryopreserved human hepatocytes were seeded and treated similarly. To study the formation and kinetics of AFB_1 metabolites, the culture medium was sampled over a time course up to 24 h and analyzed by HPLC–MS/MS. Furthermore, the DNA and the intracellular proteins were isolated and digested after 30 min, 2 h, and 24 h for the analysis of DNA (AFB_1-Gua and AFB_1-FAPY) and protein (AFB_1-Lys) adducts.

Phase II metabolites of AFB_1 were not commercially available and were prepared from AFB_1 as references for quantification by HPLC–MS/MS. AFB_1-GSH was produced enzymatically with rat liver microsomes and cytosol. AFB_1-NAC, AFB_1-Lys, and AFB_1-Gua were prepared following a chemical epoxidation of AFB_1 with DMDO.

Analysis of AFB$_1$ in the culture medium of the hepatocytes

The detected concentrations of AFB_1 in the hepatocyte cell culture media over the time course of 24 h are summarized in Fig. 3.

AFB_1 levels declined rapidly in the culture medium of mouse hepatocytes as after one hour of 1 μM incubation only 0.2 μM of AFB_1 remained and already after 6 h AFB_1 was no longer detectable. Fast conversion by mouse hepatocytes occurred also at the high concentration (10 μM), but AFB_1 was only detectable up to 6 h after incubation.

In rat hepatocyte medium AFB_1 disappeared completely within 24 h after incubation of 1 μM AFB_1. However, the decrease was slower in rats compared to mice; after 6 h a concentration of 70 nM AFB_1 remained in the culture medium of rat hepatocytes compared to the complete disappearance in that of mouse hepatocytes at this time point. In line, incubation of 10 μM AFB_1 did not result in a complete conversion by rat hepatocytes, with 3.48 μM AFB_1 remaining after 24 h. The concentration of AFB_1 in human hepatocyte medium decreased comparatively slowly as 636 nM and 8.54 μM remained after incubation of 1 μM and 10 μM of AFB_1, respectively, after 24 h.

Analysis of AFB$_1$ metabolites in mouse hepatocyte medium

AFP_1 was detected as the main metabolite of AFB_1 in mouse hepatocytes and increased within 2 h to 115 nM, followed by a decrease to 9 nM at 24 h (Fig. 4a). The same trend was observed for AFM_1 but to a lower extent. A concentration of 11 nM AFM_1 was reached after 2 h of incubation which then declined to a remaining level of 0.3 nM after 24 h. The
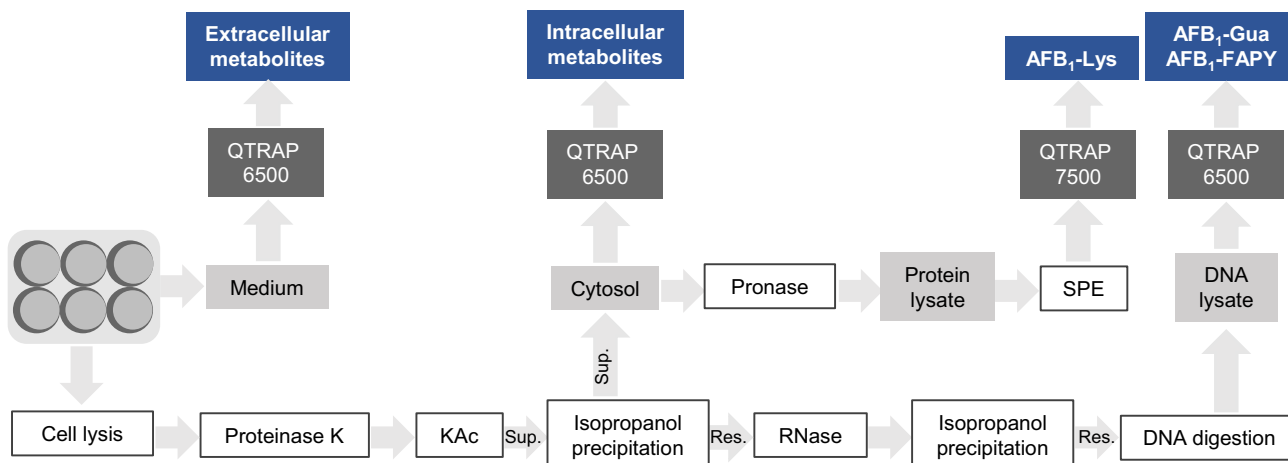

Fig. 2 Sample preparation and analyzed metabolites in the various matrices after incubation of AFB_1 in primary hepatocytes of mouse, rat, and human for 24 h (*Sup* supernatant, *Res* residue, *KAc* potassium acetate, *SPE* solid phase extraction)
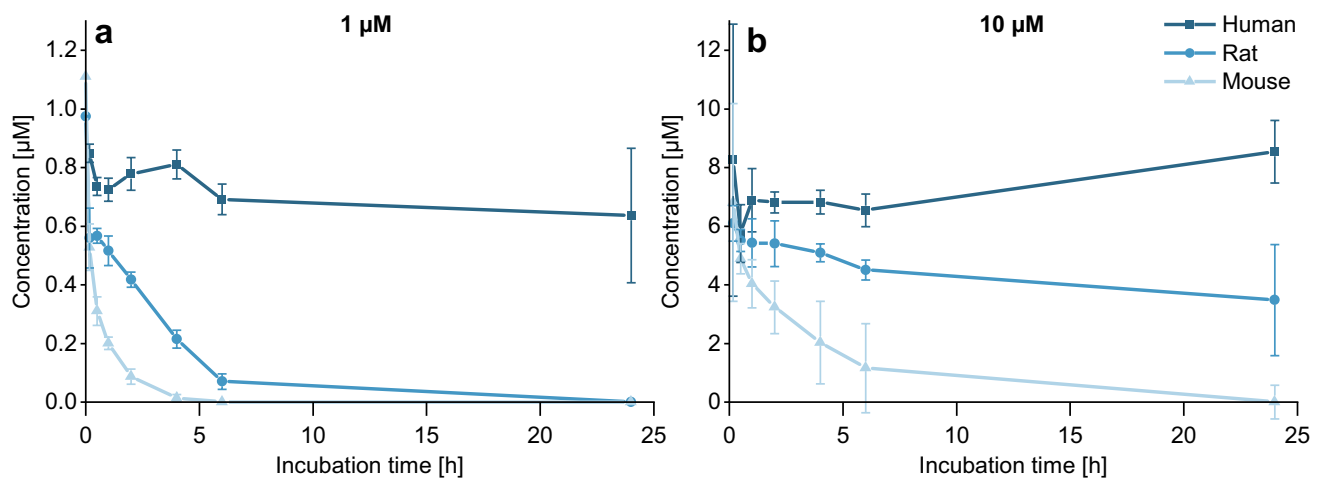
Fig. 3 AFB_1 concentration in mouse (light blue), rat (blue), and human (dark blue) hepatocyte medium after incubation of **a** 1 μM and **b** 10 μM AFB_1 over 24 h. Quantification was performed in a culture medium using HPLC–MS/MS in $n = 3 \times 2$. The 10 μM incubation of human hepatocytes was carried out in $n = 2 \times 2$

10 μM incubation gave a comparable temporal result as the two-phase I metabolites increased within the first 4 h to a maximum of 896 nM AFP_1 and 353 nM AFM_1, followed by a decrease until 24 h (Fig. 4b). The higher concentration of 10 μM also enabled the detection of AFQ_1 (Fig. 4d) which increased within the first 4 h to a maximum of 25 nM, followed by a decrease similar to the other phase I metabolites. AFL was only detected in traces after incubation of 10 μM AFB_1 and reached the highest concentration of 1 nM within 2 h, followed by a decrease until the end of the experiment (Fig. 4d). Yet another highly abundant metabolite of AFB_1 was AFB_1-GSH which increased rapidly in the first 4 h of incubation and reached maximum concentrations of 42 nM and 784 nM after incubation with 1 μM and 10 μM, respectively, at 24 h (Fig. 4a, b). AFB_1-NAC, most probably a metabolite of AFB_1-GSH, increased slowly and reached also a maximum after 24 h with quantified concentrations of 11 nM AFB_1-NAC and 191 nM AFB_1-NAC for the incubation with 1 μM AFB_1 and 10 μM AFB_1, respectively (Fig. 4a, b). AFB_1-Lys was detectable in the cell culture medium in low concentrations of up to 0.9 nM and 17 nM after 24 h of 1 μM and 10 μM AFB_1-treatment of primary mouse hepatocytes, respectively (Fig. 4c, d). AFB_1-Gua was not detected.

Analysis of AFB_1 metabolites in rat hepatocyte medium

As the main metabolite of rat hepatocytes, AFB_1-GSH was detected with increasing concentrations, reaching a plateau of 72 nM (1 μM) and 415 nM (10 μM), respectively after 6 h (Fig. 5a, b). These kinetics are similar to mouse hepatocyte metabolism (Fig. 4) while a slower increase was

observed for AFB_1-NAC, especially in the 10 μM incubation. After 24 h incubation, maximum concentrations of only 62 nM and 157 nM of 1 μM and 10 μM, respectively, were reached. The concentration of AFB_1-NAC was significantly higher in rat hepatocytes in comparison to mouse hepatocytes after 1 μM incubation, whereas the formation after 10 μM incubation was comparable. The main hydroxylated metabolite found in rat hepatocytes was AFM_1, which was also detected at higher concentrations in rat hepatocyte culture medium compared to the culture medium of mouse hepatocytes. For incubation with 1 μM AFB_1, a maximum concentration of 51 nM AFM_1 was determined after 6 h following a slight decline of the AFM_1 level down to 30 nM after 24 h (Fig. 5a). For incubations with 10 μM AFB_1, a constant increase of the AFM_1 concentration in culture medium was observed, amounting to 425 nM after 24 h (Fig. 5b). In the incubations with 10 μM AFB_1, also a second hydroxylated metabolite AFQ_1 occurred with a continuously increasing concentration, reaching 112 nM after 24 h (Fig. 5b). The other phase I metabolites AFL and AFP_1 as well as AFB_1-Gua and AFB_1-Lys were detected only in trace amounts (Fig. 5c, d).

Analysis of AFB_1 metabolites in human hepatocyte culture medium

The main metabolite of AFB_1 formed by human hepatocytes after 1 μM incubation was AFM_1 (Fig. 6a). After 24 h, concentrations of this metabolite reached maxima of 33 nM and 46 nM for 1 μM and 10 μM of AFB_1 which was much lower than the concentrations generated by the other species. In addition, also AFQ_1 was formed by human hepatocytes. However, after incubation of 1 μM, only
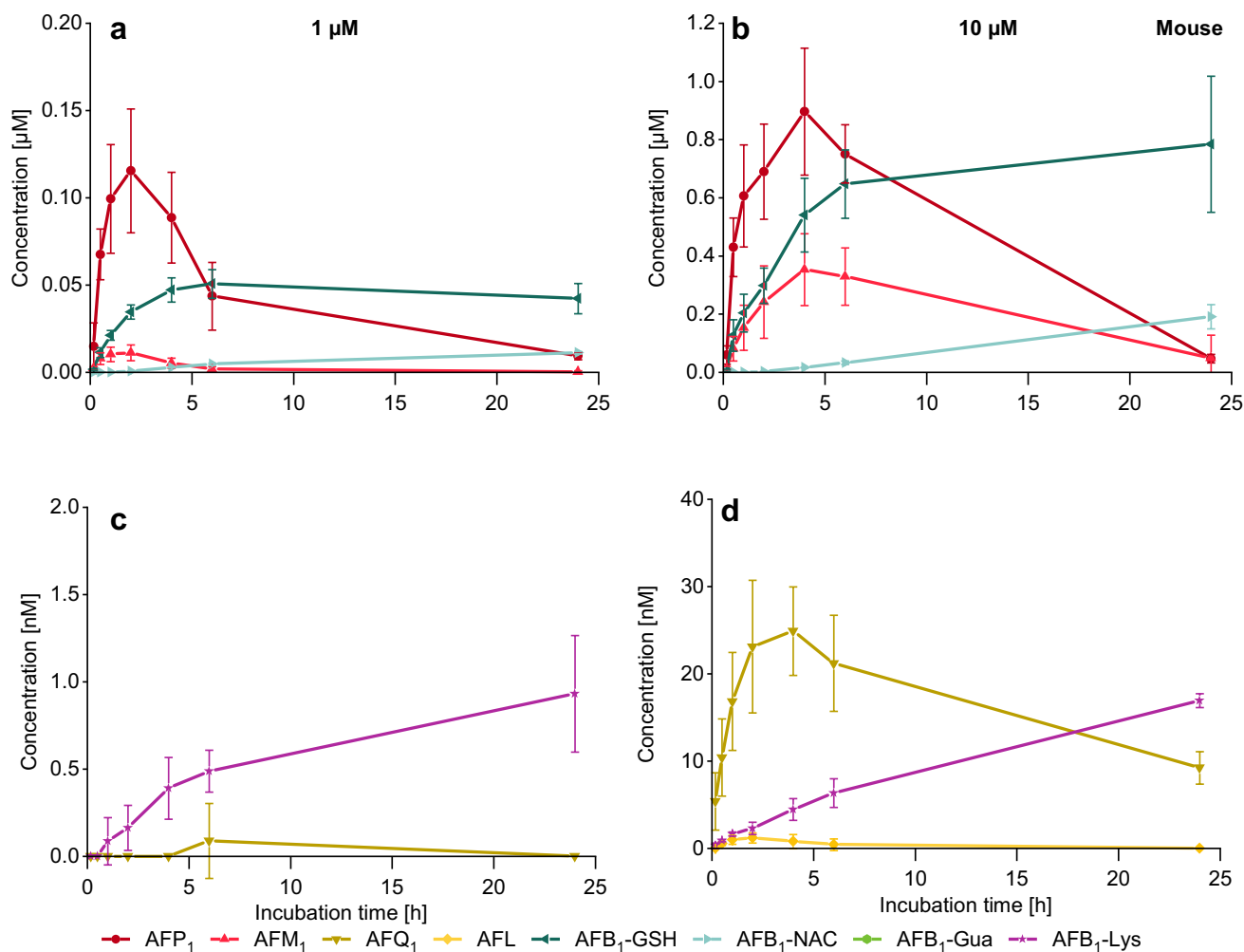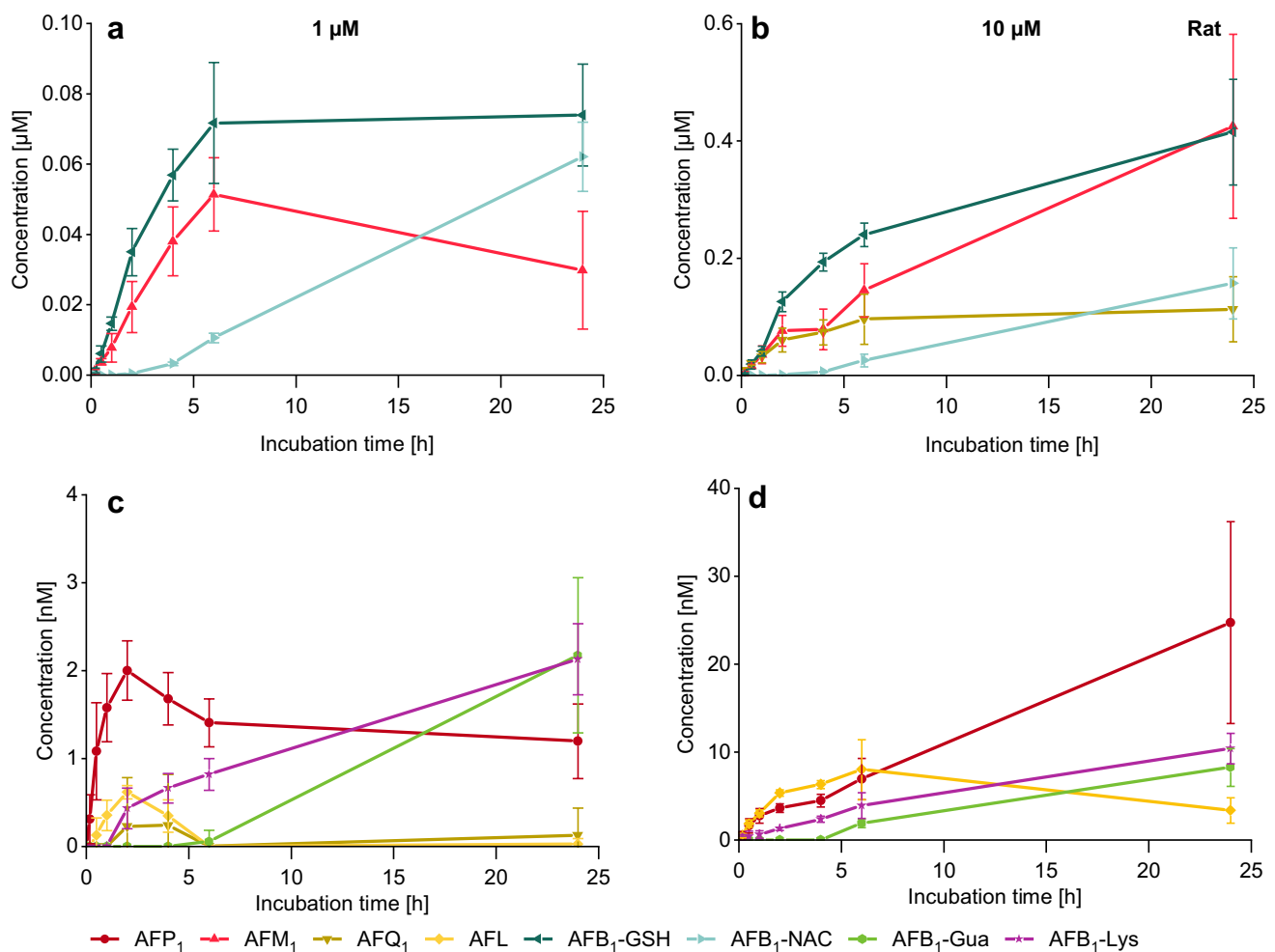
Fig. 4 Conversion of AFB_1 in primary mouse hepatocytes ($n = 3 \times 2$) analyzed in cell culture medium over 24 h via HPLC–MS/MS. The diagrams depicted in **a** and **c** relate to an incubation of 1 μM AFB_1 and **b** and **d** show the kinetics of an incubation of 10 μM AFB_1. Lev- els of AFP_1, AFM_1, AFB_1-GSH, and AFB_1-NAC shown in **a** and **b** are given in micromolar scale; those of the minor metabolites AFQ_1, AFL, and AFB_1-Lys in charts **c** and **d** are shown in nanomolar scale

2 nM AFQ_1 were detectable after 24 h (Fig. 6c). Further- more, the incubation with 10 μM AFB_1 strongly induced the formation of AFQ_1, which was generated continuously up to 52 nM within 24 h (Fig. 6b). AFL is another metabo- lite which was formed in low concentrations by rodent hepatocytes, increasing up to 50 nM, especially in the first 4 h in human cells (Fig. 6b). Afterward, the concentration remained constant until the end of the incubation period. At the lower concentration, AFB_1 (1 μM) was metabolized to 2 nM AFL within the first 4 h and remained constant up to 24 h (Fig. 6c). AFP_1 was just formed in trace amounts. Except for AFB_1-Lys, no further epoxidation-related adducts were detected. AFB_1-Lys was found in concentra- tions of 4 nM (1 μM) and 6 nM (10 μM) in the respective samples, which is comparably high (Fig. 6c, d).

Formation of adducts with macromolecules

In addition to the determination of metabolites in cell culture media, the amount of DNA adducts still bound to the DNA at specific time points was analyzed in the cell lysates (Fig. 7a). The highest adduct levels were observed in rat hepatocytes. Already after 30 min 550 AFB_1-Gua/10^8 dG (1 μM) and 734 AFB_1-Gua/10^8 dG (10 μM) were quantified. This level further increased and reached a maximum after 2 h as 1 μM of AFB_1 resulted in 589 AFB_1-Gua/10^8 dG, and the higher concentration led to a number of 1386 AFB_1-Gua/10^8 dG. At the end of the experiment, the number of DNA adducts decreased markedly to respective amounts of 446 AFB_1-Gua/10^8 dG and 1024 AFB_1-Gua/10^8 dG upon incubation of 1 μM and 10 μM AFB_1 in rat hepatocytes.

Fig. 5 Conversion of AFB_1 in primary rat hepatocytes ($n = 3 \times 2$) analyzed in cell culture medium over 24 h via HPLC–MS/MS. The diagrams depicted in **a** and **c** relate to an incubation of 1 μM AFB_1 and **b** and **d** show the kinetics of an incubation of 10 μM AFB_1. Levels of AFM_1, AFB_1-GSH, and AFB_1-NAC are shown in **a** and **b**. AFQ_1 is also formed in high yields after incubation of 10 μM AFB_1 as shown in chart **b**, and as a minor metabolite shown in chart **c** after incubation with 1 μM AFB_1. The other minor metabolites AFP_1, AFL, and AFB_1-Lys are shown in charts **c** and **d**

The formation of the DNA adduct was lower in mouse hepatocytes, and DNA adducts were only detected at the higher test concentration with a maximum after 30 min (408 AFB_1-Gua/10^8 dG), followed by a rapid decline by more than 90% between 2 and 24 h (Fig. 7a). In the lysates of human hepatocytes, AFB_1-Gua was not detected at all.

In addition to the DNA adducts, also the formation of protein adducts was determined in the cell lysates based on the amounts of AFB_1-Lys after digestion of proteins. The results are summarized in Fig. 7b. Overall, AFB_1-Lys adduct increased over time, yet contents depended upon species and AFB_1 concentration. Rat hepatocytes formed 0.8 pmol and 3.0 pmol with 1 μM and 10 μM treatment, respectively, during 24 h incubation. The amounts generated in mouse hepatocytes were different as the 1 μM incubation resulted in less AFB_1-Lys at all time points reaching a maximum

of 0.2 pmol after 24 h. The high substrate concentration resulted in higher amounts of AFB_1-Lys which were comparable to those in rat hepatocytes or even higher with a maximum of 2.6 pmol after short-term treatment. Human hepatocyte metabolism also led to the formation of AFB_1-Lys, up to amounts around 1.0 pmol at both AFB_1 concentrations.

Determination of intracellular analyte contents

In addition to the analysis of medium samples also intracellular contents of the analytes were determined (Fig. 8). The data fit the results obtained from the medium samples which showed more rapid metabolism of AFB_1 at 1 μM and 10 μM by mice than rat hepatocytes and a low conversion by human hepatocytes (Fig. 3). Accordingly, the human hepatocytes contain the highest intracellular amounts of unmetabolized
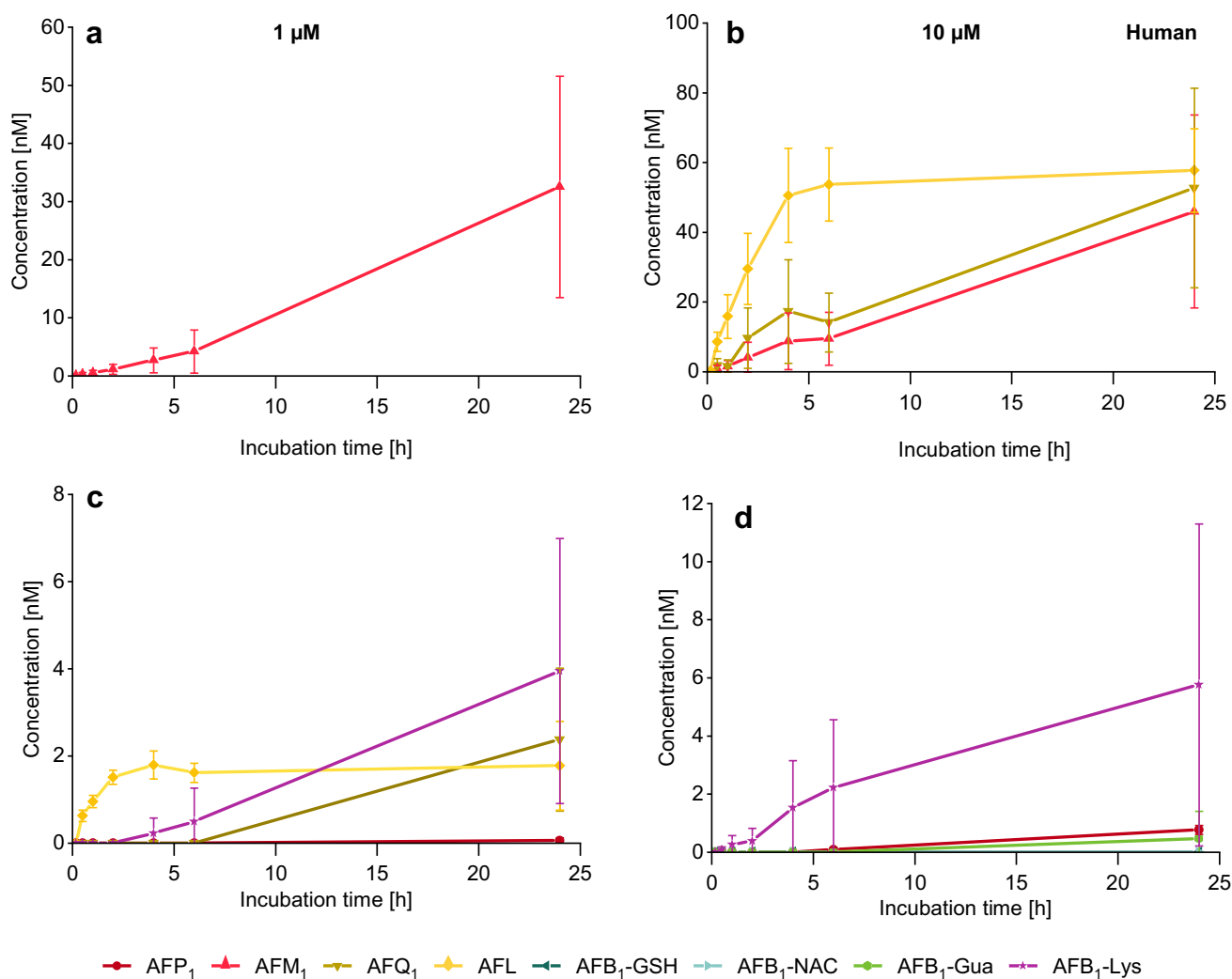
Fig. 6 Conversion of AFB$_1$ in primary human hepatocytes ($n=3\times2$) analyzed in cell culture medium over 24 h via HPLC–MS/MS. The diagrams depicted in **a** and **c** relate to an incubation of 1 μM AFB$_1$ and **b** and **d** show the kinetics of an incubation of 10 μM AFB$_1$ ($n=2\times2$). The major metabolites are given in **a** and **b** and the minor metabolites are depicted in **c** and **d**. Levels of AFM$_1$, AFQ$_1$, AFL, AFP$_1$, AFB$_1$-Gua, and AFB$_1$-Lys are given in nanomolar scale. AFB$_1$-GSH and AFB$_1$-NAC were not detected

parent compound at all sampling times (Fig. 8a). AFB$_1$, the predominant analyte in all samples, was present at high levels over the whole time-course in human hepatocytes, while in rat and mouse the intracellular AFB$_1$ content decreased considerably until the end of the experiment. The level of intracellular metabolites increased over time (Fig. 8b, c), and a pattern with some distinct differences between species was observed. For example, AFL, AFQ$_1$, and AFM$_1$ appeared as major metabolites in human hepatocytes, but AFB$_1$-GSH was the major metabolite in rodent hepatocytes, along with AFP$_1$ and AFM$_1$ in mice, or AFM$_1$ and AFQ$_1$ in rats. The main metabolites of all species were already present after 30 min regardless of the incubated AFB$_1$ concentration. Similar to the medium samples, human hepatocytes only formed low amounts of metabolites, and AFB$_1$-GSH was not detected.

Discussion

The toxicity of AFB$_1$ is dependent on bioactivation and detoxication pathways (Fig. 1) and of considerable interest in light of well-known interspecies differences in susceptibility to acute and chronic effects of AFB$_1$ (Eaton and Gallagher 1994; Hengstler et al. 1999). The present study has applied advanced analytical methods to elucidate AFB$_1$ conversion by hepatocytes of three species to characterize phase I and phase II metabolites in the medium or intracellular as well as macromolecule (DNA, protein) bound products.

Cellular uptake and conversion rate of AFB$_1$

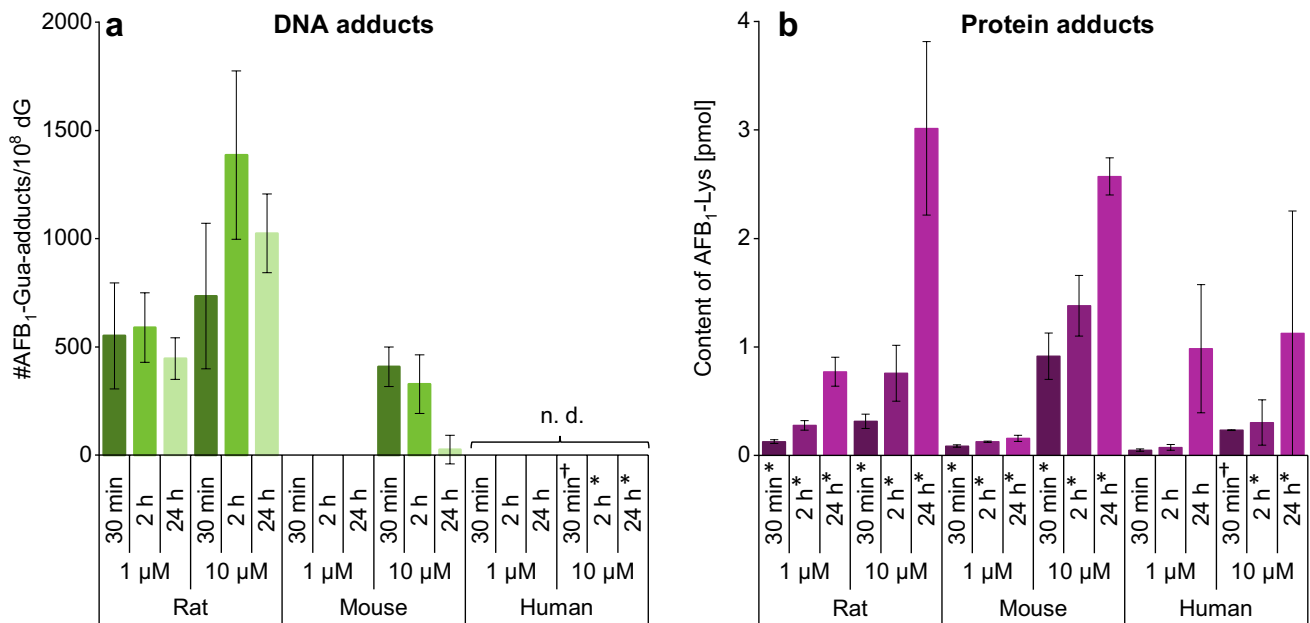AFB$_1$ was transported rapidly into the hepatocytes as the compound occurred intracellularly in high levels in all

Fig. 7 AFB$_1$-Gua detected in the DNA **a** and AFB$_1$-Lys in proteins **b** after cell lysis at 30 min, 2 h, and 24 h ($n = 3 \times 2$). Differing numbers of replicates are marked: $*n = 2 \times 2$, $†n = 1 \times 2$. The AFB$_1$-Gua data are normalized to the 2'-deoxyguanosine (dG) concentration, *n.d.* not detected

species already after 30 min (Fig. 8). Based on previously reported volumes of hepatocytes ranging between 3 pL and 6.8 pL (Wiśniewski et al. 2016; Swift et al. 2010; Chatterjee et al. 2014), the intracellular concentrations of AFB$_1$ were estimated. In all species, a strong enrichment of up to 1 mM (human cells) compared to the medium concentrations was calculated for the 10 μM AFB$_1$ incubation. Hanigan and Laishes (1984) showed a rapid uptake of radiolabeled [^{3}H]-AFB$_1$ by primary rat and mouse hepatocytes. The intracellular radioactivity increased more rapidly in rat than in mouse hepatocytes and remained constant over 4 h. In contrast, the radioactivity in mouse hepatocytes decreased after 30 min and the maximum level was not as high as in rat hepatocytes (Hanigan and Laishes 1984). The data shown here led to similar conclusions as the maximum cellular AFB$_1$ level in mouse hepatocytes was significantly lower than in rat and human cells (Fig. 8a). Furthermore, the intracellular levels of AFB$_1$ increased for up to 2 h in rats and in human hepatocytes, while in mouse hepatocytes the highest level was observed at the first determined time-point of 30 min. The decrease in AFB$_1$ levels in rodent hepatocytes after 2 h was in line with the formation of intracellular metabolites (Fig. 8c) and an efficient efflux of the metabolites to the cell culture medium. AFB$_1$ contents in human hepatocytes decreased slightly between 2 and 24 h while low levels of intracellular metabolites were formed over time (Fig. 8b). A low rate of conversion was also reflected in the culture medium with high remaining AFB$_1$ levels up to 24 h (Fig. 3). Notably, (unavoidable) differences in isolation and cultivation

procedures may affect hepatocyte viability or metabolic competence. Rodent hepatocytes are prepared from freshly isolated livers by common perfusion procedures (Godoy et al. 2013, Appendix 1). Human liver on the other hand is rarely available and usually removed *post mortem* before hepatocyte isolation, which is most commonly performed from slices of the liver rather than the whole organ. Due to infrequent accessibility, it is more common to cryopreserve human hepatocytes and thaw these cells before the actual experiment. These methodical differences need to be taken into consideration when comparing the quantitative data of biological samples from different species origins. The activity of selected enzymes in primary human hepatocytes is just slightly affected by cryopreservation, but the cultivation time can affect enzyme activity. The activities of CYP 1A2 and 3A4, which catalyze AFB$_1$ metabolism in human hepatocytes, are known to decrease with longer adherent cultivation time (Smith et al. 2012; Li et al. 1999; Hewitt et al. 2007; Deng et al. 2018; Wilson et al. 1997; Langouet et al. 1995). Nonetheless, human hepatocytes used in our study were found to form AFL along with AFQ$_1$, AFM$_1$, AFB$_1$-Gua, and AFB$_1$-Lys.

Comparing the conversion of AFB$_1$ in the three species, the data show that independent of the concentration used (1 μM or 10 μM), the metabolism of AFB$_1$ in mice hepatocytes is the fastest followed by rats and humans (Fig. 3). Analysis of AFB$_1$ metabolism showed distinct differences in metabolite patterns that confirm and expand knowledge on bioactivation and detoxication pathways in these three species.
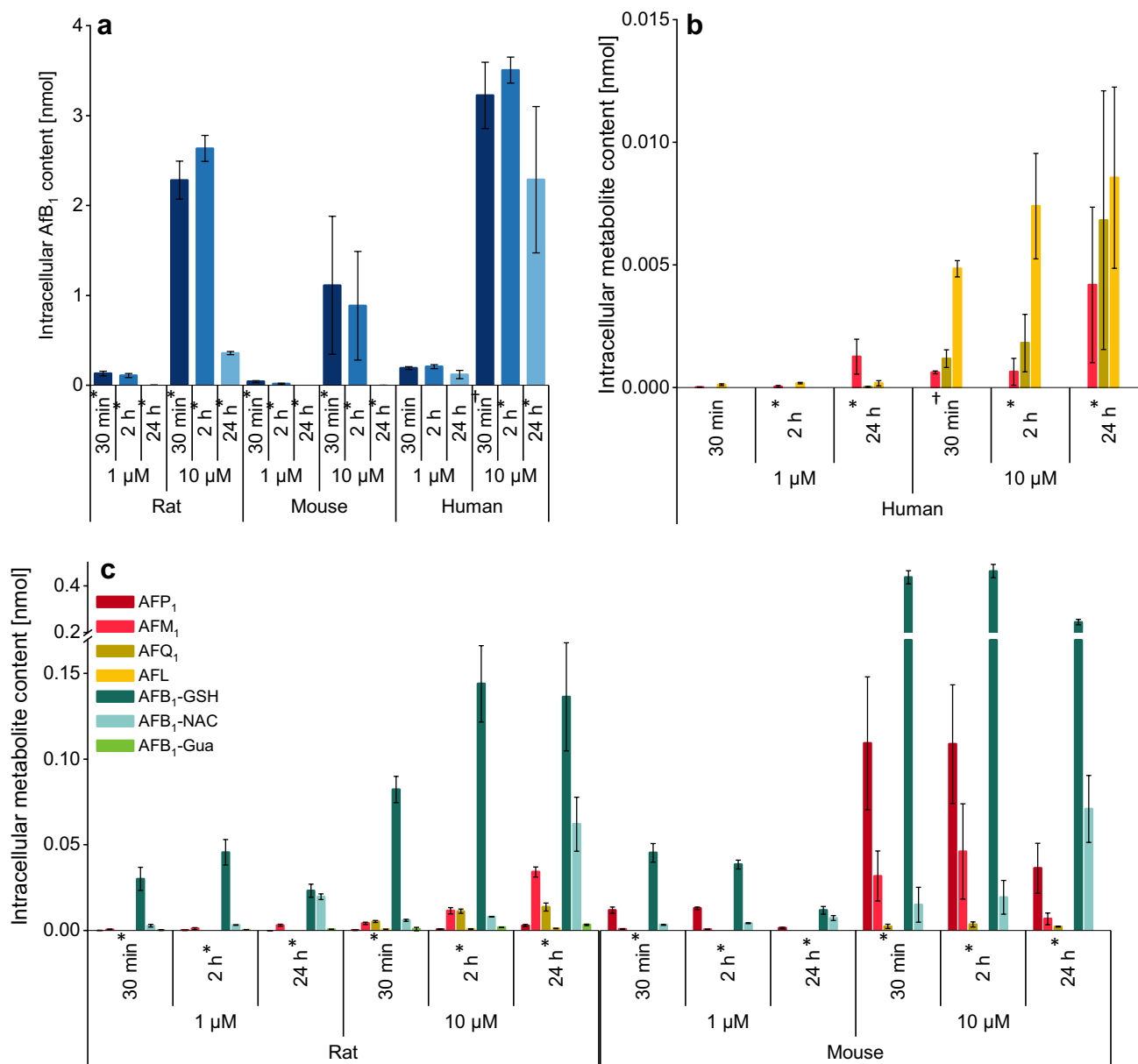
Fig. 8 Intracellular contents of AFB$_1$ **a** and its metabolites in primary human **b** mouse and rat hepatocytes **c** at 30 min, 2 h, and 24 h in $n = 3 \times 2$ numbers of replicates or as marked: $*n = 2 \times 2$ and $†n = 1 \times 2$

Metabolite pattern of phase I metabolism

In mouse hepatocytes, AFB$_1$ was predominantly converted to **AFP$_1$** (Fig. 4) in the first hours while the formation of AFP$_1$, the *O*-demethylation product of AFB$_1$, was significantly lower in the other two species (Figs. 5, 6). Also for other compounds, harmine, scoparone, and 6-methoxy-3-(3′,4′,5′-trimethoxy-benzoyl)-1*H*-indole, a faster *O*-demethylation has been reported for mice compared to rats and humans (Fayyaz et al. 2018; Burke and Upshall 1976; Yao et al. 2007). Fayyaz et al. (2018) suggested CYP2A isoforms to be involved in this demethylation reaction. Early experiments

on AFB$_1$ metabolism by liver microsomes indicated that the formation of AFP$_1$ is preferred in mice compared to rats and humans (Ramsdell and Eaton 1990; Degen and Neumann 1981; Dahms and Gurtoo 1976). The conversion to AFP$_1$ is considered as an effective way of detoxifying AFB$_1$, as this metabolite is far less toxic shown in fertile chicken eggs and in newborn mice (Buchi et al. 1973; Stoloff et al. 1972). Yet, there were some hints on the formation of AFP$_1$-DNA adducts in vivo in rat liver (Croy and Wogan 1981; Essigmann et al. 1982). More recent studies on the toxicity of AFP$_1$ are not available and its cytotoxicity on human cells has not been investigated. The highest levels of AFP$_1$ were

seen after short-term incubation of rodent hepatocytes, followed by a strong decrease (Fig. 4) occurring mainly in mice which is possibly related to further metabolism of AFP_1 in phase II reactions. In an attempt to identify these conjugated metabolites AFP_1 glucuronide (AFP_1-Glc) was detected via HPLC-HRMS in about 100-fold higher levels in the mouse samples than in the rat samples. In human samples no AFP_1-Glc was detectable. The data are shown in Figure S6 in Online Resource 1. A glucuronidation of AFP_1 and sulfation have been shown previously (Dalezios et al. 1971; Eaton et al. 1988).

The main phase I metabolite of rat hepatocytes was **AFM_1** (Fig. 5) which confirms an early report on the presence of AFM_1 together with AFQ_1 as major hydroxylated metabolites formed by rat liver post-mitochondrial supernatants (Degen and Neumann 1981). AFM_1 was also found in cultured mouse and human hepatocytes (Figs. 4, 6) and was also the main metabolite of human hepatocytes treated with 1 μM of AFB_1. This phase I metabolite occurs also in human and animal milk as well as in dairy products and is a relevant contaminant in human nutrition (Min et al. 2020; Iqbal et al. 2015). AFM_1 exerts a slightly lower cytotoxic potency than AFB_1 in various cell systems (Gao et al. 2022; Wu et al. 2021; Green et al. 1982). Therefore, AFM_1 formation is less effective as a detoxification pathway than conversion to AFP_1. An epoxidation of AFM_1 can result in DNA adduct formation and mutagenicity. However, the formation of DNA adducts and genotoxicity of AFM_1 was lower compared to AFB_1 (Bujons et al. 1995; Loveland et al. 1988; Lutz et al. 1980; Egner et al. 2003).

Along with AFM_1 and AFL, **AFQ_1** was one of the main metabolites of human hepatocytes (Figs. 6, 8b) and was formed mainly at 10 μM incubation of AFB_1. In contrast to AFM_1, which is formed by CYP1A2 following Michaelis–Menten kinetics, AFQ_1 is formed by CYP3A4 which follows Hill kinetics resulting in differences in AFB_1 metabolite pattern at higher substrate levels (Gallagher et al. 1996; Ueng et al. 1995). According to these models, CYP3A4 is activated only at higher concentrations leading to effective formation of AFQ_1 at 10 μM AFB_1 and low activity upon incubation at 1 μM AFB_1. This effect was observed in rat as well as in human hepatocytes (Figs. 5, 6, 8) and also described previously in human and rat microsomes (Ramsdell and Eaton 1990). In mouse hepatocytes, small amounts of AFQ_1 were formed upon incubation of 10 μM AFB_1 (Fig. 4). AFQ_1 exerts far lower acute toxicity and mutagenicity than AFB_1, and its carcinogenic potency in rainbow trout is about 1% of AFB_1 (Eaton and Gallagher 1994). Also with metabolic activation of AFQ_1, a mutagenic potency of only 1% relative to AFB_1 was observed (Wong and Hsieh 1976). Therefore, AFQ_1 formation was identified as an important detoxification pathway metabolite for humans, as it was found in human hepatocyte incubations (at similar levels as

AFM_1) at high AFB_1 concentrations. AFQ_1 has been found in urine and fecal samples along with AFM_1 and AFB_1-Gua of Chinese males (Mykkänen et al. 2005). Thus, AFQ_1 could be used as a biomarker for human AFB_1 exposure together with AFM_1, AFB_1-Gua, and AFB_1-Lys (Vidal et al. 2018).

Interestingly, **AFL** was formed most efficiently by human hepatocytes and was also the predominant intracellular metabolite at the high (10 μM) incubation concentration (Figs. 6, 8b). AFL is generated by a cytosolic reductase and an interconversion to AFB_1 is described (Wong et al. 1979). Therefore, this metabolite acts as a reservoir for AFB_1, which implicates high relevance in toxicity (Rushing and Selim 2019; Wong et al. 1979) as it also binds to DNA in rainbow trout with similar efficiency compared to AFB_1 (Loveland et al. 1988). Taking into account that AFL is transferred across the placenta and is also formed by placental tissue, this metabolic pathway is of special interest for the developmental toxicity of AFB_1 (Partanen et al. 2010).

Bioactivation of AFB_1 and subsequent reactions

In addition to the above-mentioned phase I reactions, AFB_1 is epoxidized at the double bond of the furofuran ring. The *exo*-epoxide is known to be responsible for the mutagenicity and cytotoxicity of AFB_1 due to its high reactivity and binding to DNA and to proteins, with the latter occurring via a reactive AFB_1-dialdehyde formed from AFB_1-epoxide (van Vleet et al. 2002; Kärenlampi 1987; Sabbioni et al. 1987). On the other hand, AFB_1-epoxide can undergo inactivation reactions by phase II enzymes.

The epoxide is detoxified via enzymatic conjugation with glutathione to **AFB_1-GSH** (Fig. 1). This metabolite was formed in mouse and rat hepatocytes with comparable kinetics (Figs. 4, 5) despite differences in glutathione S-transferase (GST) isozymes responsible for this reaction (Deng et al. 2018). In contrast, human hepatocytes did not form the AFB_1-GSH adduct (Fig. 6), which is in line with previous experiments where AFB_1-epoxide was conjugated with GSH in the presence of mouse cytosol but not with human cytosol (Neal et al. 1998), and in vitro studies with subcellular fractions of rat, mouse, and human origin (Ramsdell and Eaton 1990; Raney et al. 1992a; Moss and Neal 1985). The importance of detoxification via glutathione conjugation was shown by Ilic and colleagues who studied the toxicity of AFB_1 in mGSTA3 knock-out mice. These mice showed strong hepatic necrosis and had 100-fold higher levels of DNA adducts (AFB_1-N^7-Gua) than wild-type mice (Ilic et al. 2010). This result is also relevant for humans who have a poor ability to detoxify AFB_1-epoxide in the liver by glutathione conjugation (Guengerich et al. 1996; Raney et al. 1992b).

The glutathione adduct is apparently further metabolized to **AFB_1-NAC** in mouse and rat hepatocytes with a

short time delay in relation to AFB_1-GSH adduct formation. This metabolite has been detected also in isolated rat liver hepatocyte incubations with radiolabeled [^{3}H-]AFB_1 (Ch'ih et al. 1991). Furthermore, some degradation products of AFB_1-GSH such as AFB_1-Cys-Gly, AFB_1-Cys-Gln, and AFB_1-Cys were identified by HPLC-HRMS in the medium of mice and rat hepatocytes after 24 h culture. The AFB_1-Cys-Gly metabolite was previously detected in the urine of rats along with other more prominent biomarkers of AFB_1-exposure (Walton et al. 2001).

To investigate the bioactivation of AFB_1, DNA was isolated from the cells and the formation of **AFB_1-Gua** was determined. The rat hepatocytes formed higher amounts of AFB_1-Gua compared to mouse and human hepatocytes (Fig. 7a). The adduct level in rat hepatocytes showed an increase between 30 min and 2 h and remained at a high level up to 24 h (at about 70% compared to 2 h). In mouse hepatocytes, the highest level was quantified at 30 min but declined within 24 h to less than 10% of the initial amounts, which indicated efficient removal of AFB_1-Gua from DNA. Recently, spatio-temporal intravital imaging of AFB_1 in mice revealed fast uptake from the sinusoidal blood by hepatocytes, and only transient enrichment in hepatocyte nuclei followed by rapid clearance into bile canaliculi (Ghallab et al. 2021). This observation could be related to differences in metabolism and faster DNA repair activity of mouse hepatocytes compared to rats (Bedard et al. 2005). In human hepatocytes, no DNA adducts were detectable in the DNA lysates; however, bioactivation was nevertheless indicated by small amounts of AFB_1-Gua in the medium (Fig. 6d). Considering the rather low conversion rate by human hepatocytes in this study, the presence of this product in the culture medium and also AFB_1-Lys adduct formation (Figs. 6, 7) are clear evidence for AFB_1-epoxidation. Cole et al. (1986) compared DNA adduct formation in primary hepatocytes from mice, rats, and human origin incubated with 200 nM [^{3}H-]AFB_1 and compared its binding to DNA with liquid scintillation counting. In contrast to the data shown here, they could not differentiate between formed adducts. Furthermore, cultivation procedures differed between species, and differences in conversion rates of AFB_1 need also to be taken into consideration. Nevertheless, they also measured the highest DNA binding in hepatocytes of male rats and only small amounts in mice. The difference between the two rodent species is in line with the data presented here. The DNA adduct formation in rats and mice was reported in numerous publications and the carcinogenicity of AFB_1 was already described to be far higher for rats than for mice (Woo et al. 2011; Coskun et al. 2019; Croy et al. 1978).

The AFB_1-epoxide can be hydrolyzed to AFB_1-dihydrodiol, formed spontaneously or catalyzed by epoxide hydrolases, and epoxide hydrolysis led to some reduction in the genotoxicity of AFB_1 (Johnson et al. 1997). The AFB_1-dihydrodiol is unstable and can rearrange pH-dependently to AFB_1-dialdehyde which reacts with the ε-amino group of lysine residues in proteins (see Fig. 1) (Sabbioni et al. 1987). This product was determined in the present investigation as **AFB_1-Lys** after protein digestion (Fig. 7b). Its presence in all three species already after short incubation shows that all hepatocytes are capable of an efficient epoxidation of AFB_1. Species and time-dependent differences in AFB_1-Lys content may be related to differences in the expression and activity of epoxide hydrolases in mice, rats, and humans (Thomas et al. 1990). Moreover, GSH-conjugation of AFB_1 epoxide is likely to affect the fraction which is hydrolyzed and then results in the formation of protein adducts. While all metabolites of AFB_1 were generated at rather low levels in human hepatocytes, AFB_1-Lys formation was of similar magnitude as in rodent hepatocytes. This result can be related to missing GSH conjugation in human cells and an effective enolization of AFB_1-epoxide. Because of an accumulation of bioactivated AFB_1 in proteins, AFB_1-Lys is also used as a long-term biomarker of human aflatoxin exposure (Sabbioni et al. 1987; Wild et al. 1990; Turner et al. 1998).

Studies on the cytotoxicity of AFB_1 in rodent species showed that rat hepatocytes are more sensitive than mouse hepatocytes and accumulate also far more [^{3}H-]AFB_1 bound to macromolecules (Hanigan and Laishes 1984). This finding can be now interpreted better considering the new data presented here on the rapid metabolism of AFB_1 in mouse hepatocytes, mainly to AFP_1 which is less toxic, an efficient DNA repair of AFB_1-Gua, and efficient detoxification of the epoxide via glutathione conjugation. Rat hepatocytes metabolize AFB_1 slower, mainly to AFM_1 and AFQ_1. While AFB_1-epoxide is also converted to AFB_1-GSH, the levels of DNA adduct and protein binding are higher in rat than in mouse. A considerable part of incubated AFB_1 was not recovered, which might be due to the further metabolism of phase I metabolites such as glucuronidation of AFP_1 and degradation of AFB_1-GSH. Other reported metabolites of AFB_1 such as AFB_{2a}, aflatoxicol M_1, or aflatoxicol H_1 (Unger et al. 1977; Salhab and Hsieh 1975; Salhab et al. 1977) as well as AFB_1-dihydrodiol, dialdehyde, and dialcohol were not quantified in this study.

The distinct metabolite patterns, including human hepatocytes, are summarized in Fig. 9 and reflect different enzyme activities involved in phase I and phase II metabolism of AFB_1 not only in different species but also in different concentrations. For easier comparison of the kinetics, the formation rates of all compounds in the cell culture medium were calculated and are presented in Table S21 in Online Resource 1.

Fig. 9 Metabolite pattern and remaining AFB$_1$ calculated according to the results in cell culture medium after the incubation of mouse, rat, and human hepatocytes with 1 μM and 10 μM AFB$_1$ for 4 h
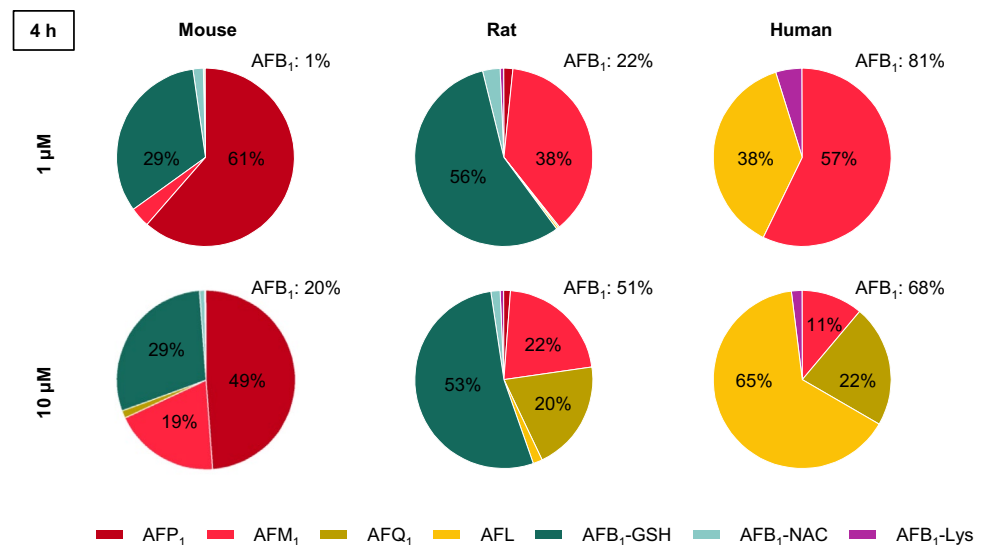
Conclusions

The species-specific differences in susceptibility towards AFB$_1$ treatment were related to variations in metabolism in previous studies. Therefore, a comprehensive study on phase I and phase II metabolism of AFB$_1$ as well as the binding to macromolecules in mouse, rat, and human primary hepatocytes was conducted using HPLC–MS/MS analysis.

The fastest conversion of AFB$_1$ was observed in mouse hepatocytes which formed AFP$_1$ as the main hydroxylated metabolite with some qualitative evidence for its glucuronidation. Efficient glutathione conjugation of the epoxide contributed to comparatively low binding to DNA and proteins, which is in line with better repair of DNA lesions and low toxicity of AFB$_1$ in this species. In contrast, rat hepatocytes formed high amounts of protein and DNA adducts although glutathione conjugation appeared to be similar to mice. Also, AFM$_1$ which exerts higher toxicity than AFP$_1$ was detected as a major phase I metabolite in rat hepatocytes as well as in human cells. The formation of AFQ$_1$ was observed at high substrate concentrations in rat and human hepatocytes. AFL occurs mainly in human cells and is probably of high relevance for toxicity. Missing or poor detoxication by glutathione conjugation favored DNA and protein adduct formation in accord with the known high toxicity and mutagenicity in the human liver. The analysis showed that the overall metabolite pattern of the three species is hardly comparable. Moreover, it was demonstrated that in addition to glutathione conjugation, also phase I metabolism significantly contributes to detoxication and species susceptibility of AFB$_1$.

The comprehensive analysis using advanced methodology confirms early results on the metabolism of AFB$_1$. Because of the high sensitivity and selectivity of HPLC–MS/MS measurements, more specific insights were obtained into the toxification and detoxification pathways of AFB$_1$. This is the first study comparing the metabolism of AFB$_1$ comprehensively in mice, rats, and humans in primary hepatocytes considering the quantification of a multitude of metabolites as well as the binding of AFB$_1$ to macromolecules.

Declarations

References

Alekseyev YO, Hamm ML, Essigmann JM (2004) Aflatoxin B1 formamidopyrimidine adducts are preferentially repaired by the nucleotide excision repair pathway in vivo. Carcinogenesis 25(6):1045–1051. https://doi.org/10.1093/carcin/bgh098

Bedard LL, Alessi M, Davey S, Massey TE (2005) Susceptibility to aflatoxin B$_1$-induced carcinogenesis correlates with tissue-specific differences in DNA repair activity in mouse and in rat. Cancer Res 65(4):1265–1270. https://doi.org/10.1158/0008-5472.CAN-04-3373

Buchi G, Spitzner D, Paglialunga S, Wogan GN (1973) Synthesis and toxicity evaluation of aflatoxin P$_1$. Life Sci 13(8):1143–1149. https://doi.org/10.1016/0024-3205(73)90381-0

Bujons J, Hsieh DP, Kado NY, Messeguer A (1995) Aflatoxin M$_1$ 8,9-epoxide: preparation and mutagenic activity. Chem Res Toxicol 8(3):328–332. https://doi.org/10.1021/tx00045a002

Burke MD, Upshall DG (1976) Species and phenobarbitone-induced differences in the kinetic constants of liver microsomal harmine O-demethylation. Xenobiotica 6(5):321–328. https://doi.org/10.3109/00498257609151643

Cenis JL (1992) Rapid extraction of fungal DNA for PCR amplification. Nucleic Acids Res 20(9):2380. https://doi.org/10.1093/nar/20.9.2380

Chatterjee S, Bijsmans ITGW, van Mil SWC, Augustijns P, Annaert P (2014) Toxicity and intracellular accumulation of bile acids in sandwich-cultured rat hepatocytes: role of glycine conjugates. Toxicol in Vitro 28(2):218–230. https://doi.org/10.1016/j.tiv.2013.10.020

Ch'ih JJ, Biedrzycka DW, Devlin TM (1991) Isolated hepatocytes are capable of excreting aflatoxin metabolites. Biochem Biophys Res Commu 178(3):1002–1007. https://doi.org/10.1016/0006-291X(91)90991-F

Cole KE, Hsu IC, Trump BF (1986) Comparative ultrastructural effects of aflatoxin B1 on mouse, rat, and human hepatocytes in primary culture. Cancer Res 46(3):1290–1296

Coskun E, Jaruga P, Vartanian V, Erdem O, Egner PA, Groopman JD, Lloyd RS, Dizdaroglu M (2019) Aflatoxin-guanine DNA adducts and oxidatively induced DNA damage in aflatoxin-treated mice in Vivo as measured by liquid chromatography-tandem mass spectrometry with isotope dilution. Chem Res Toxicol 32(1):80–89. https://doi.org/10.1021/acs.chemrestox.8b00202

Croy RG, Wogan GN (1981) Temporal patterns of covalent DNA adducts in rat liver after single and multiple doses of aflatoxin B1. Cancer Res 41(1):197–203

Croy RG, Essigmann JM, Reinhold VN, Wogan GN (1978) Identification of the principal aflatoxin B$_1$-DNA adduct formed in vivo in rat liver. Proc Natl Acad Sci U S A 75(4):1745–1749. https://doi.org/10.1073/pnas.75.4.1745

Dahms R, Gurtoo HL (1976) Metabolism of aflatoxin B$_1$ to aflatoxins Q$_1$, M$_1$ and P$_1$ by mouse and rat. Res Commun Chem Pathol Pharmacol 15(1):11–20

Dalezios J, Wogan GN, Weinreb SM (1971) Aflatoxin P$_1$: a new aflatoxin metabolite in monkeys. Science 171(3971):584–585. https://doi.org/10.1126/science.171.3971.584

Degen GH, Neumann H-G (1978) The major metabolite of aflatoxin B$_1$ in the rat is a glutathione conjugate. Chem-Biol Interact 22(2–3):239–255. https://doi.org/10.1016/0009-2797(78)90129-1

Degen GH, Neumann HG (1981) Differences in aflatoxin B$_1$-susceptibility of rat and mouse are correlated with the capability in vitro to inactivate aflatoxin B$_1$-epoxide. Carcinogenesis 2(4):299–306. https://doi.org/10.1093/carcin/2.4.299

Deng J, Zhao L, Zhang N-Y, Karrow NA, Krumm CS, Qi D-S, Sun L-H (2018) Aflatoxin B1 metabolism: Regulation by phase I and II metabolizing enzymes and chemoprotective agents. Mutat Res, Rev Mutat Res 778:79–89. https://doi.org/10.1016/j.mrrev.2018.10.002

Dohnal V, Wu Q, Kuča K (2014) Metabolism of aflatoxins: key enzymes and interindividual as well as interspecies differences. Arch Toxicol 88(9):1635–1644. https://doi.org/10.1007/s00204-014-1312-9

Eaton DL, Gallagher EP (1994) Mechanisms of aflatoxin carcinogenesis. Annu Rev Pharmacol Toxicol 34:135–172. https://doi.org/10.1146/annurev.pa.34.040194.001031

Eaton DL, Monroe DH, Bellamy G, Kalman DA (1988) Identification of a novel dihydroxy metabolite of aflatoxin B$_1$ produced in vitro and in vivo in rats and mice. Chem Res Toxicol 1(2):108–114. https://doi.org/10.1021/tx00002a004

EFSA Contam PANEL (2020) Scientific opinion-Risk assessment of aflatoxins in food. EFSA 18(3):e06040. https://doi.org/10.2903/j.efsa.2020.6040

Egner PA, Yu X, Johnson JK, Nathasingh CK, Groopman JD, Kensler TW, Roebuck BD (2003) Identification of aflatoxin M$_1$–N^7-guanine in liver and urine of tree shrews and rats following administration of aflatoxin B1. Chem Res Toxicol 16(9):1174–1180. https://doi.org/10.1021/tx034106u

Essigmann JM, Croy RG, Nadzan AM, Busby WF, Reinhold VN, Büchi G, Wogan GN (1977) Structural identification of the major DNA adduct formed by aflatoxin B1 in vitro. Proc Natl Acad Sci U S A 74(5):1870–1874. https://doi.org/10.1073/pnas.74.5.1870

Essigmann JM, Croy RG, Bennet RA, Wogan GN (1982) Metabolic activation of aflatoxin B$_1$: patterns of DNA adduct formation, removal, and excretion in relation to carcinogenesis. Drug Metab Rev 13(4):581–602

Fayyaz A, Makwinja S, Auriola S, Raunio H, Juvonen RO (2018) Comparison of In Vitro hepatic scoparone 7-O-demethylation between humans and experimental animals. Planta Med 84(5):320–328. https://doi.org/10.1055/s-0043-119886

Gallagher EP, Kunze KL, Stapleton PL, Eaton DL (1996) The kinetics of aflatoxin B$_1$ oxidation by human cDNA-expressed and human liver microsomal cytochromes P450 1A2 and 3A4. Toxicol Appl Pharmac 141(2):595–606. https://doi.org/10.1006/taap.1996.0326

Gao Y-N, Yang X, Wang J-Q, Liu H-M, Zheng N (2022) Multi-omics reveal additive cytotoxicity effects of aflatoxin B1 and aflatoxin M1 toward intestinal NCM460 cells. Toxins 14(6):368. https://doi.org/10.3390/toxins14060368

Ghallab A, Hassan R, Myllys M, Albrecht W, Friebel A, Hoehme S, Hofmann U, Seddek A-L, Braeuning A, Kuepfer L, Cramer B, Humpf H-U, Boor P, Degen GH, Hengstler JG (2021) Subcellular spatio-temporal intravital kinetics of aflatoxin B1 and ochratoxin A in liver and kidney. Arch Toxicol 95(6):2163–2177. https://doi.org/10.1007/s00204-021-03073-5

Godoy P, Hewitt NJ, Albrecht U et al (2013) Recent advances in 2D and 3D in vitro systems using primary hepatocytes, alternative

hepatocyte sources and non-parenchymal liver cells and their use in investigating mechanisms of hepatotoxicity, cell signaling and ADME. Arch Toxicol 87(8):1315–1530. https://doi.org/10.1007/s00204-013-1078-5

Green CE, Rice DW, Hsieh DP, Byard JL (1982) The comparative metabolism and toxic potency of aflatoxin B_1 and aflatoxin M_1 in primary cultures of adult-rat hepatocytes. Food Chem Toxicol 20(1):53–60. https://doi.org/10.1016/s0278-6915(82)80009-4

Guengerich FP, Johnson WW, Ueng YF, Yamazaki H, Shimada T (1996) Involvement of cytochrome P450, glutathione S-transferase, and epoxide hydrolase in the metabolism of aflatoxin B1 and relevance to risk of human liver cancer. Environ Health Perspect 104(Suppl 3):557–562. https://doi.org/10.1289/ehp.96104s3557

Guengerich FP, Johnson WW, Shimada T, Ueng YF, Yamazaki H, Langouët S (1998) Activation and detoxication of aflatoxin B1. Mutat Res 402(1–2):121–128. https://doi.org/10.1016/S0027-5107(97)00289-3

Hanigan HM, Laishes BA (1984) Toxicity of aflatoxin B_1 in rat and mouse hepatocytes *in vivo* and *in vitro*. Toxicology 30(3):185–193. https://doi.org/10.1016/0300-483x(84)90090-8

Hengstler JG, van der Burg B, Steinberg P, Oesch F (1999) Interspecies differences in cancer susceptibility and toxicity. Drug Metab Rev 31(4):917–970. https://doi.org/10.1081/dmr-100101946

Hewitt NJ, Lechón MJG, Houston JB et al (2007) Primary hepatocytes: current understanding of the regulation of metabolic enzymes and transporter proteins, and pharmaceutical practice for the use of hepatocytes in metabolism, enzyme induction, transporter, clearance, and hepatotoxicity studies. Drug Metab Rev 39(1):159–234. https://doi.org/10.1080/03602530601093489

Ilic Z, Crawford D, Vakharia D, Egner PA, Sell S (2010) Glutathione-S-transferase A3 knockout mice are sensitive to acute cytotoxic and genotoxic effects of aflatoxin B1. Toxicol Appl Pharmacol 242(3):241–246. https://doi.org/10.1016/j.taap.2009.10.008

Iqbal SZ, Jinap S, Pirouz AA, Ahmad Faizal AR (2015) Aflatoxin M_1 in milk and dairy products, occurrence and recent challenges: a review. Trends Food Sci Technol 46(1):110–119. https://doi.org/10.1016/j.tifs.2015.08.005

Johnson WW, Yamazaki H, Shimada T, Ueng YF, Guengerich FP (1997) Aflatoxin B1 8,9-epoxide hydrolysis in the presence of rat and human epoxide hydrolase. Chem Res Toxicol 10(6):672–676. https://doi.org/10.1021/tx960209j

Kärenlampi SO (1987) Mechanism of cytotoxicity of aflatoxin B1: role of cytochrome P1–450. Biochem Biophys Res Commu 145(2):854–860. https://doi.org/10.1016/0006-291x(87)91043-6

Kensler TW, Roebuck BD, Wogan GN, Groopman JD (2011) Aflatoxin: a 50-year odyssey of mechanistic and translational toxicology. Toxicol Sci 120(Suppl 1):S28-48. https://doi.org/10.1093/toxsci/kfq283

Langouet S, Brian Coles B, Morel F, Becquemont L, Beaune P, Guengerich FP (1995) Inhibition of CYP1A2 and CYP3A4 by oltipraz results in reduction of aflatoxin B1 metabolism in human hepatocytes in primary culture. Cancer Res 55:5574–5579

Li AP, Lu C, Brent JA, Pham C, Fackett A, Ruegg CE, Silber PM (1999) Cryopreserved human hepatocytes: characterization of drug-metabolizing enzyme activities and applications in higher throughput screening assays for hepatotoxicity, metabolic stability, and drug-drug interaction potential. Chem-Biol Interact 121(1):17–35. https://doi.org/10.1016/s0009-2797(99)00088-5

Loveland PM, Wilcox JS, Hendricks JD, Bailey GS (1988) Comparative metabolism and DNA binding of aflatoxin B_1, aflatoxin M_1, aflatoxicol and aflatoxicol-M_1 in hepatocytes from rainbow trout (*Salmo gairdneri*). Carcinogenesis 9(3):441–446. https://doi.org/10.1093/carcin/9.3.441

Lutz WK, Jaggi W, Lüthy J, Sagelsdorff P, Schlatter C (1980) In vivo covalent binding of aflatoxin B_1 and aflatoxin M_1 to liver DNA of rat, mouse and pig. Chem-Biol Interact 32(3):249–256. https://doi.org/10.1016/0009-2797(80)90092-7

McCoy LF, Scholl PF, Schleicher RL, Groopman JD, Powers CD, Pfeiffer CM (2005) Analysis of aflatoxin B1-lysine adduct in serum using isotope-dilution liquid chromatography/tandem mass spectrometry. Rapid Commun Mass Spectrom 19(16):2203–2210. https://doi.org/10.1002/rcm.2045

McHugh TE, Atkins WM, Racha JK, Kunze KL, Eaton DL (1996) Binding of the aflatoxin-glutathione conjugate to mouse glutathione S-transferase A3–3 is saturated at only one ligand per dimer. J Biol Chem 271(44):27470–27474. https://doi.org/10.1074/jbc.271.44.27470

Min L, Li D, Tong X, Sun H, Chen W, Wang G, Zheng N, Wang J (2020) The challenges of global occurrence of aflatoxin M_1 contamination and the reduction of aflatoxin M_1 in milk over the past decade. Food Control 117:107352. https://doi.org/10.1016/j.foodcont.2020.107352

Moss EJ, Neal GE (1985) The metabolism of aflatoxin B_1 by human liver. Biochem Pharmacol 34(17):3193–3197. https://doi.org/10.1016/0006-2952(85)90170-4

Moss EJ, Judah DJ, Przybylski M, Neal GE (1983) Some mass-spectral and n.m.r. analytical studies of a glutathione conjugate of aflatoxin B1. Biochem J 1(210):227–233

Moss EJ, Neal GE, Judah DJ (1985) The mercapturic acid pathway metabolites of a glutathione conjugate of aflatoxin B_1. Chem-Biol Interact 55:139–155. https://doi.org/10.1016/S0009-2797(85)80124-1

Murcia HW, Diaz GJ (2021) Protective effect of glutathione *S*-transferase enzyme activity against aflatoxin B_1 in poultry species: relationship between glutathione *S*-transferase enzyme kinetic parameters, and resistance to aflatoxin B_1. Poult Sci 100(8):101235. https://doi.org/10.1016/j.psj.2021.101235

Mykkänen H, Zhu H, Salminen E, Juvonen RO, Ling W, Ma J, Polychronaki N, Kemiläinen H, Mykkänen O, Salminen S, El-Nezami H (2005) Fecal and urinary excretion of aflatoxin B_1 metabolites (AFQ_1, AFM_1 and AFB-N[7]-guanine) in young Chinese males. Int J Cancer 115(6):879–884. https://doi.org/10.1002/ijc.20951

Neal GE, Colley PJ (1979) The formation of 2,3-dihydro-2,3-dihydroxy aflatoxin B_1 by the metabolism of aflatoxin B_1 in vitro by rat liver microsomes. FEBS Lett 101(2):382–386. https://doi.org/10.1016/0014-5793(79)81049-2

Neal GE, Eaton DL, Judah DJ, Verma A (1998) Metabolism and toxicity of aflatoxins M_1 and B_1 in human-derived *in vitro* systems. Toxicol Appl Pharmac 151(1):152–158. https://doi.org/10.1006/taap.1998.8440

Partanen HA, El-Nezami HS, Leppänen JM, Myllynen PK, Woodhouse HJ, Vähäkangas KH (2010) Aflatoxin B1 transfer and metabolism in human placenta. Toxicol Sci 113(1):216–225. https://doi.org/10.1093/toxsci/kfp257

Raj HG, Lotlikar PD (1984) Urinary excretion of thiol conjugates of aflatoxin B_1 in rats and hamsters. Cancer Lett 22(2):125–133. https://doi.org/10.1016/0304-3835(84)90109-5

Ramsdell HS, Eaton DL (1990) Species susceptibility to aflatoxin B_1 carcinogenesis: comparative kinetics of microsomal biotransformation. Cancer Res 50(3):615–620

Raney KD, Meyer DJ, Ketterer B, Harris TM, Guengerich FP (1992a) Glutathione conjugation of aflatoxin B_1 *exo*- and *endo*-epoxides by rat and human glutathione *S*-transferases. Chem Res Toxicol 5:470–478

Raney KD, Meyer DJ, Ketterer B, Harris TM, Guengerich FP (1992b) Glutathione conjugation of aflatoxin B_1 *exo*- and *endo*-epoxides by rat and human glutathione *S*-transferases. Chem Res Toxicol 5(4):470–478. https://doi.org/10.1021/tx00028a004

Renaud JB, Walsh JP, Sumarah MW (2022) Simplified synthesis and stability assessment of aflatoxin B_1-lysine and aflatoxin G_1-lysine. Toxins 14(56):1–18. https://doi.org/10.3390/toxins14010056

Roebuck BD, Wogan GN (1977) Species comparison of in vitro metabolism of aflatoxin B1. Cancer Res 37(6):1649–1656

Rushing BR, Selim MI (2019) Aflatoxin B1: a review on metabolism, toxicity, occurrence in food, occupational exposure, and detoxification methods. Food Chem Toxicol 124:81–100. https://doi.org/10.1016/j.fct.2018.11.047

Sabbioni G, Skipper PL, Büchi G, Tannenbaum SR (1987) Isolation and characterization of the major serum albumin adduct formed by aflatoxin B_1 in vivo in rats. Carcinogenesis 8(6):819–824. https://doi.org/10.1093/carcin/8.6.819

Salhab AS, Hsieh DP (1975) Aflatoxicol H1: a major metabolite of aflatoxin B1 produced by human and rhesus monkey livers in vitro. Res Commun Chem Pathol Pharmacol 10(3):419–429

Salhab AS, Abramson FP, Geelhoed GW, Edwards GS (1977) Aflatoxicol M_1, a new metabolite of aflatoxicol. Xenobiotica 7(7):401–408. https://doi.org/10.3109/00498257709035799

Sass CD, Vincenzi Jager A, Gustavo Tonin F, Naira Zambelli Ramalho L, Silva Ramalho F, Gomes Constantino M, Augusto Fernandes Oliveira C (2013) Methods for chemical preparation of aflatoxin B 1 adducts, AFB 1 -N 7 -guanine and AFB 1 -lysine. Toxin Reviews 32(4):68–74. https://doi.org/10.3109/15569543.2013.852110

Smela ME, Hamm ML, Henderson PT, Harris CM, Harris TM, Essigmann JM (2002) The aflatoxin B_1 formamidopyrimidine adduct plays a major role in causing the types of mutations observed in human hepatocellular carcinoma. Proc Natl Acad Sci U S A 99(10):6655–6660. https://doi.org/10.1073/pnas.102167699

Smith CM, Nolan CK, Edwards MA, Hatfield JB, Stewart TW, Ferguson SS, LeCluyse EL, Sahi J (2012) A comprehensive evaluation of metabolic activity and intrinsic clearance in suspensions and monolayer cultures of cryopreserved primary human hepatocytes. J Pharm Sci 101(10):3989–4002. https://doi.org/10.1002/jps.23262

Stoloff L, Verrett MJ, Dantzman J, Reynaldo EF (1972) Toxicological study of aflatoxin P_1 using the fertile chicken egg. Toxicol Appl Pharmac 23(3):528–531. https://doi.org/10.1016/0041-008x(72)90055-5

Swift B, Pfeifer ND, Brouwer KLR (2010) Sandwich-cultured hepatocytes: an in vitro model to evaluate hepatobiliary transporter-based drug interactions and hepatotoxicity. Drug Metab Rev 42(3):446–471. https://doi.org/10.3109/03602530903491881

Taber DF, DeMatteo PW, Hassan RA (2013) Simplified preparation of dimethyldioxirane (DMDO). Org Synth 90:350. https://doi.org/10.15227/orgsyn.090.0350

Thomas H, Schladt L, Doehmer J, Knehr M, Oesch F (1990) Rat and human liver cytosolic epoxide hydrolases: evidence for multiple forms at level of protein and mRNA. Environ Health Perspect 88:49–55. https://doi.org/10.1289/ehp.908849

Turner PC, Dingley KH, Coxhead J, Russell S, Garner CR (1998) Detectable levels of serum aflatoxin B1-albumin adducts in the United Kingdom population: implications for aflatoxin-B1 exposure in the United Kingdom. Cancer Epidemiol Biomarkers Prev 7(5):441–447

Ueng YF, Shimada T, Yamazaki H, Guengerich FP (1995) Oxidation of aflatoxin B_1 by bacterial recombinant human cytochrome P450 enzymes. Chem Res Toxicol 8(2):218–225. https://doi.org/10.1021/tx00044a006

Unger PD, Mehendale HM, Hayes AW (1977) Hepatic uptake and disposition of aflatoxin B_1 in isolated perfused rat liver. Toxicol Appl Pharmac 41(3):523–534. https://doi.org/10.1016/s0041-008x(77)80007-0

van Vleet TR, Klein PJ, Coulombe RA (2002) Metabolism and cytotoxicity of aflatoxin B_1 in cytochrome p-450-expressing human lung cells. J Toxicol Environ Health A 65(12):853–867. https://doi.org/10.1080/00984100290071216

Vidal A, Mengelers M, Yang S, de Saeger S, de Boevre M (2018) Mycotoxin Biomarkers of exposure: a comprehensive review. Compr Rev Food Sci Food Saf 17(5):1127–1155. https://doi.org/10.1111/1541-4337.12367

Vidyasagar T, Sujatha N, Sashidhar RB (1997) Direct synthesis of aflatoxin B_1–N^7 guanine adduct: a reference standard for biological monitoring of dietary aflatoxin exposure in molecular epidemiological studies. Food Addit Contam 14(5):457–467. https://doi.org/10.1080/02652039709374552

Walton M, Egner P, Scholl PF, Walker J, Kensler TW, Groopman JD (2001) Liquid chromatography electrospray-mass spectrometry of urinary aflatoxin biomarkers: characterization and application to dosimetry and chemoprevention in rats. Chem Res Toxicol 14(7):919–926. https://doi.org/10.1021/tx010063a

Wild CP, Jiang YZ, Sabbioni G, Chapot B, Montesano R (1990) Evaluation of methods for quantitation of aflatoxin-albumin adducts and their application to human exposure assessment. Cancer Res 50(2):245–251

Wilson AS, Williams DP, Davis CD, Tingle MD, Park BK (1997) Bioactivation and inactivation of aflatoxin B_1 by human, mouse and rat liver preparations: effect on SCE in human mononuclear leucocytes. Mutat Res 373(2):257–264. https://doi.org/10.1016/s0027-5107(96)00205-9

Wiśniewski JR, Vildhede A, Norén A, Artursson P (2016) In-depth quantitative analysis and comparison of the human hepatocyte and hepatoma cell line HepG2 proteomes. J Proteomics 136:234–247. https://doi.org/10.1016/j.jprot.2016.01.016

Wong JJ, Hsieh DP (1976) Mutagenicity of aflatoxins related to their metabolism and carcinogenic potential. Proc Natl Acad Sci U S A 73(7):2241–2244. https://doi.org/10.1073/pnas.73.7.2241

Wong ZA, Decad GM, Byard JL, Hsieh DP (1979) Conversion of aflatoxicol to aflatoxin B_1 in rats in vivo and in primary hepatocyte culture. Food Cosm Toxicol 17(5):481–486. https://doi.org/10.1016/0015-6264(79)90007-5

Woo LL, Egner PA, Belanger CL, Wattanawaraporn R, Trudel LJ, Croy RG, Groopman JD, Essigmann JM, Wogan GN, Bouhenguel JT (2011) Aflatoxin B_1-DNA adduct formation and mutagenicity in livers of neonatal male and female B6C3F1 mice. Toxicol Sci 122(1):38–44. https://doi.org/10.1093/toxsci/kfr087

Wu K, Jia S, Zhang J, Zhang C, Wang S, Rajput SA, Sun L, Qi D (2021) Transcriptomics and flow cytometry reveals the cytotoxicity of aflatoxin B_1 and aflatoxin M_1 in bovine mammary epithelial cells. Ecotoxicol Environ Saf 209:111823. https://doi.org/10.1016/j.ecoenv.2020.111823

Yao H-T, Wu Y-S, Chang Y-W, Hsieh H-P, Chen W-C, Lan S-J, Chen C-T, Chao Y-S, Chang L, Sun H-Y, Yeh T-K (2007) Biotransformation of 6-methoxy-3-(3',4',5'-trimethoxy-benzoyl)-1H-indole (BPR0L075), a novel antimicrotubule agent, by mouse, rat, dog, and human liver microsomes. Drug Metab Dispos 35(7):1042–1049. https://doi.org/10.1124/dmd.106.014597

Yourtee DM, Bean TA, Kirk-Yourtee CL (1987) Human aflatoxin B1 metabolism: An investigation of the importance of aflatoxin Q1 as a metabolite of hepatic post-mitochondrial fraction. Toxicol Lett 38(3):213–224. https://doi.org/10.1016/0378-4274(87)90002-6